Biological Psychiatry: CNNI

Review

Transdiagnostic In Vivo Magnetic Resonance Imaging Markers of Neuroinflammation

Lena K.L. Oestreich and Michael J. O'Sullivan

ABSTRACT

Accumulating evidence suggests that inflammation is not limited to archetypal inflammatory diseases such as multiple sclerosis, but instead represents an intrinsic feature of many psychiatric and neurological disorders not typically classified as neuroinflammatory. A growing body of research suggests that neuroinflammation can be observed in early and prodromal stages of these disorders and, under certain circumstances, may lead to tissue damage. Traditional methods to assess neuroinflammation include serum or cerebrospinal fluid markers and positron emission tomography. These methods require invasive procedures or radiation exposure and lack the exquisite spatial resolution of magnetic resonance imaging (MRI). There is, therefore, an increasing interest in noninvasive neuroimaging tools to evaluate neuroinflammation reliably and with high specificity. While MRI does not provide information at a cellular level, it facilitates the characterization of several biophysical tissue properties that are closely linked to neuroinflammatory processes. The purpose of this review is to evaluate the potential of MRI as a noninvasive, accessible, and cost-effective technology to image neuroinflammation across neurological and psychiatric disorders. We provide an overview of current and developing MRI methods used to study different aspects of neuroinflammation and weigh their strengths and shortcomings. Novel MRI contrast agents are increasingly able to target inflammatory processes directly, therefore offering a high degree of specificity, particularly if used in conjunction with multitissue, biophysical diffusion MRI compartment models. The capability of these methods to characterize several aspects of the neuroinflammatory milieu will likely push MRI to the forefront of neuroimaging modalities used to characterize neuroinflammation transdiagnostically.

https://doi.org/10.1016/j.bpsc.2022.01.003

In recent years, compelling evidence has accumulated to suggest that psychiatric and neurological disorders are accompanied by immune system dysregulation and inflammation (1). Heightened inflammatory response has, in turn, been linked to recurrent and prolonged periods of illness and symptom severity. Inflammation is a physiological response triggered by a wide range of injurious or infectious agents, stress, and physical trauma (2). It facilitates the removal of damaged tissue and controls the recovery of tissue structure and function. Most inflammatory responses are acute and constructive, occurring in the order of seconds to hours (3). Yet, under certain circumstances, inflammation can become chronic and contribute to central nervous system (CNS) pathology (1).

Inflammation of the CNS is termed "neuroinflammation" to reflect properties that are unique to the context of the nervous system. Under normal conditions, the brain parenchyma is separated from systemic circulation by the blood-brain barrier (BBB). The BBB is a highly selective semipermeable barrier that includes endothelial cells linked by tight junctions, which prevent many large molecules and cell types from crossing into the CNS. Pathological processes, however, can induce selective changes in BBB permeability. For example, in response to injury, a cascade of inflammatory processes are initiated that disrupt the segregation of the two systems, allowing inflammatory cells and mediators to cross into the CNS (4). The innate, or nonspecific, immune response provides a first line of defense against pathogens and consists of sentinel cells, such as activated microglia, the resident macrophages of the CNS, which are the first responders to tissue damage in injured brain regions (5). Microglial activation is typically accompanied by the release of inflammatory mediators such as proinflammatory cytokines and chemokines, which are also produced by endothelial cells. Chemokines on endothelial cells interact with blood-borne leukocytes to enhance affinity for their endothelial ligands (Figure 1A) (6). This in turn changes BBB permeability by impairing the expression of BBB integrity molecules, enabling leukocytes to migrate across endothelial cells into the CNS (7). These inflammatory processes are accompanied by the release of reactive oxygen species into the extracellular space where macrophages, microglia, and astrocytes mediate immune defense and the production of excitotoxic metabolites causes further tissue damage (8). Increased BBB permeability enables the entrance of T and B lymphocytes into the brain, which are the hallmark of the adaptive immune response (6). Adaptive immunity is specific to antigens present. While typically targeted at foreign pathogens, adaptive immunity can erroneously attack endogenous antigens, leading to autoimmune disorders. In white matter, prolonged neuroinflammation damages oligodendrocytes and myelin sheaths (Figure 1C) (5).

© 2022 Society of Biological Psychiatry. Published by Elsevier Inc. This is an open access article under the CC BY license (http://creativecommons.org/licenses/by/4.0/).

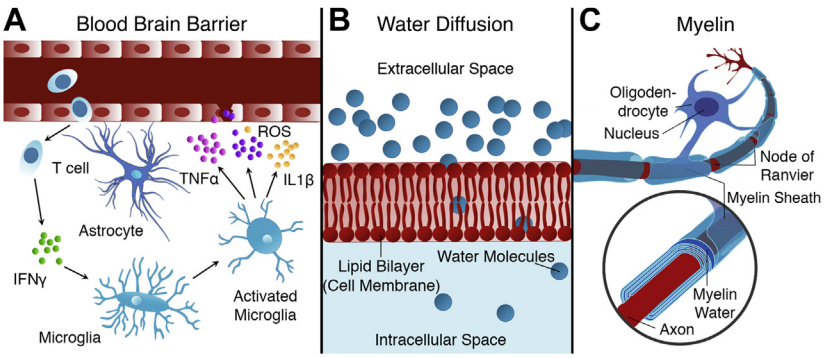

Figure 1. Cellular processes associated with neuroinflammation. **(A)** Severe cases of neuroinflammation can lead to blood-brain barrier breakdown: activated microglia and astrocytes emit proinflammatory cytokines, such as TNFα and IL1β. Proinflammatory cytokines induce excessive osmosis of intracellular water into the extraneuronal space, where neurotoxic molecules such as ROS induce breakdown of the blood-brain barrier. This enables the entrance of T cells into the brain, which further promotes the expression of proinflammatory cytokines such as IFNγ and microglia activation, eliciting a reciprocal reinforcement of neuroinflammatory and neurodegenerative processes. **(B)** Neuroinflammation, through extravasation of fluid, leads to an increase of extracellular free-water. **(C)** In white matter, prolonged neuroinflammation leads to an unwrapping of the myelin sheath. IFNγ, interferon gamma; IL1β, interleukin 1β; ROS, reactive oxygen species; TNFα, tumor necrosis factor α.

White matter pathology and neuroinflammation can also be observed distal from injury, with evidence of propagation along white matter pathways (9).

Neuroinflammation is the key feature of inflammatory neurological disorders such as multiple sclerosis and meningoencephalitis (10). However, recent evidence suggests that secondary inflammation in response to injury may also play a role in neurological disorders not typically classified as inflammatory, such as Alzheimer's disease, stroke, or traumatic brain injury (TBI) (10). Moreover, neuroinflammation has been reported as an important mechanism in the development of several psychiatric disorders (11). Neurological and psychiatric disorders are highly comorbid. Combined with the substantial prevalence of neuroinflammation in disorders of the nervous system (12), neuroinflammatory processes have significant transdiagnostic relevance for illness monitoring and novel treatment strategies.

Several characteristics of the brain present substantial challenges for the identification and quantification of neuroinflammation (13). Molecules cannot cross the BBB, making it difficult to develop imaging agents that can reach the brain. Furthermore, the skull prevents direct access to the brain, rendering diagnostic procedures such as biopsies and therapeutic surgical interventions more hazardous. Magnetic resonance imaging (MRI) is a noninvasive, readily accessible, and cost-effective technology without the need for invasive procedures or radioactive agents. While MRI is unable to image immune cells or molecular targets directly, it offers the opportunity to characterize several processes tightly coupled with inflammation. This field is rapidly advancing, and several methods have been developed to image inflammation-related processes with MRI, yet their specificity to neuroinflammation and generalizability across disorders need to be established. Here, we review the available literature on noninvasive MRI proxies of neuroinflammation in vivo, studied across neurological and psychiatric disorders. We will determine the benefits of each method in the context of different illnesses and assess their potential use to image neuroinflammation transdiagnostically.

METHODS

Reviewed MRI methods include contrast-enhanced MRI (CE-MRI), structural MRI, and diffusion MRI as well as new analysis approaches derived from these acquisitions. Search terms, a detailed description of each method, and validation studies supporting their use to yield measures sensitive to neuroinflammation are provided in the Supplement. The databases PubMed, PsycINFO, and Web of Science were searched for relevant articles published within a 10-year period between March 2011 and August 2021. To be eligible for inclusion, studies had to 1) include clinical cohorts defined by the search terms, 2) be conducted in adult (18 years+) human cohorts, 3) be written in English, 4) use at least one MRI method defined by the search terms, 5) be original research (i.e., no case studies, reviews, or meta-analysis), and 6) provide a quantifiable estimate of neuroinflammation. MRI markers of neuroinflammation were scored against validation criteria for each study (Table 1).

RESULTS

A total of 21,574 records were identified, of which 82 studies reported data on neuroinflammatory markers derived from MRI in one or multiple neurological or psychiatric disorders (Figure 2). After initial review, studies using T2-weighted or fluid-attenuated inversion recovery (FLAIR) were excluded owing to the limited specificity of measures used to index neuroinflammation (a summary of T2 and FLAIR studies is provided in Tables S1 and S2). The final results include 54 studies.

MRI Markers Sensitive to BBB Permeability: CE-MRI

Gadolinium-Based CE-MRI. Identified neurological studies were conducted in stroke (14–27), TBI (28,29), and Parkinson's disease (30) (Table 2). In studies investigating stroke, neuroinflammation was indirectly inferred from BBB permeability (18–24,27) and intracranial plaque enhancement (15–17,24–26). Culprit plaques had a higher degree of contrast enhancement than asymptomatic plaques (15,25), likely reflecting increased inflammatory activity in these regions. Meningeal lymphatic vessels provide direct connections between the CNS and the peripheral immune system. Using gadolinium (Gd)-based CE-MRI employing a black-blood sequence, a study by Ding *et al.* (30) found that relative to patients with atypical Parkinsonian disorders, patients with idiopathic Parkinson's disease exhibited significantly reduced

Table 1. Criteria for Validation of MRI Markers of Neuroinflammation

Score	Definition	Rationale
0	No additional measures of inflammation	MRI markers can only be assumed to measure neuroinflammation, which is based on previous research.
1	Other measures of inflammation included but associations with MRI markers have not been tested or are assumed to measure consequences of inflammation instead of inflammation per se	In the absence of statistical comparisons between MRI markers and other measures of inflammation, interpretations are speculative. Studies testing association between inflammation markers and structural estimates derived from MRI test effects of inflammation on brain structure rather than the validity of MRI markers sensitive to neuroinflammation.
2	Associations between peripheral markers of inflammation and MRI markers	Associations with systemic inflammation may indicate that the MRI marker measures inflammation, but the association can also be caused by other common mechanisms or third variables.
3	Associations between CSF markers of inflammation and MRI markers	CSF markers can quantify inflammation in the central nervous system, narrowing down associations of MRI markers with neuroinflammation specifically. However, CSF markers cannot be extracted from distinct brain regions, making it impossible to localize inflammation within the brain and only providing partial validation of MRI markers.
4	Molecular imaging of inflammation (e.g., optical imaging, PET, MRS) coincides with elevated levels of MRI markers within a circumscribed brain region	Accumulation of a contrast agent that binds to microglia, myeloperoxidase, or other cells relevant for immune regulation, concurring with increased levels of the MRI marker, provides evidence that the MRI marker measures the inflammatory process specific to the imaging agent.
5	Postmortem tissue inflammation at site of enhanced MRI marker	Postmortem immunohistochemistry can quantify the presence of a large range of immune cells and processes. If performed in a region found to exhibit elevated levels of the MRI marker, associations between the MRI marker and specific immune processes can be validated.

CSF, cerebrospinal fluid; MRI, magnetic resonance imaging; MRS, magnetic resonance spectroscopy; PET, positron emission tomography.

flow through meningeal lymphatic vessels along the sigmoid and superior sagittal sinuses. Immunohistology performed on a mouse model of Parkinson's disease in the same study revealed strong meningeal inflammation and loss of tight junctions among meningeal lymphatic endothelial cells. While not providing direct evidence, the authors concluded that these pathologies may be the result of meningeal inflammation and macrophages (30). Cho *et al.* (28) used Gd-enhanced MRI to assess BBB disruption caused by TBI in younger (19–35 years) and older (60–89 years) adults. While TBI-related vascular injuries on MRI decreased from 72% at 48 hours after TBI to 32% at 1 week after TBI in younger adults, this was not the case for older adults (75%–76%). In parallel, younger patients showed greater expression of inflammatory regulatory genes at both time points and older patients were found to possess reduced activity of growth factor genes (28). Another study in TBI found meningeal injury identified on Gd-enhanced MRI to be associated with genes linked to inflammatory mediators and phagocytosis and concluded that acute inflammatory activation occurs in response to injury to the meninges after concussion (29).

Only one identified study used Gd-enhanced CE-MRI to investigate neuroinflammation related to psychiatric symptoms by comparing patients with multiple sclerosis with and without depression (31). While evidence for an increased peripheral immune-inflammatory potential was observed in patients with depression, Gd-enhanced lesions were found to be negatively associated with depression (31) (Table 2).

It has been clearly established that Gd-based CE-MRI can detect BBB breakdown in inflammatory lesions in primary inflammatory disorders of the CNS, such as multiple sclerosis. However, the available literature suggests that it is not sensitive enough to detect inflammation in CNS disorders without overt injury to the brain. This is likely because Gd-based CE-

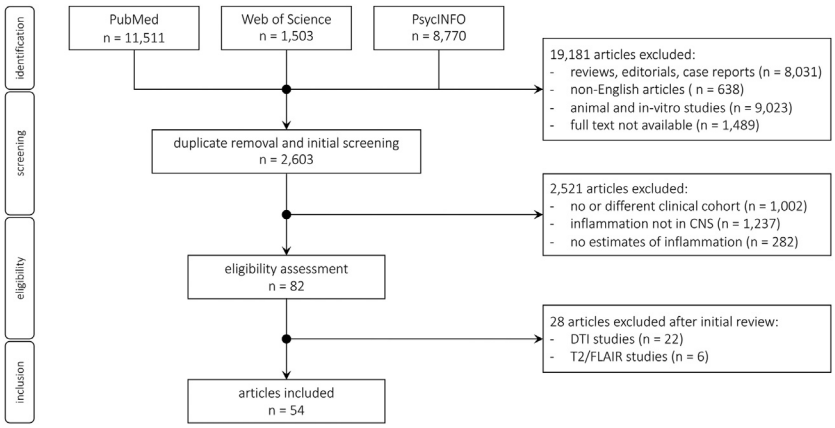

Figure 2. Flowchart of studies included in the review. CNS, central nervous system; DTI, diffusion tensor imaging; FLAIR, fluid-attenuated inversion recovery.

Table 2. Studies in Neurological and Psychiatric Disorders Using Gd-Based CE-MRI to Study Neuroinflammation

Study	Sample	Design and Analysis	Results and Conclusions	Validation
Neurological Disorders: Stroke				
Ford *et al.*, 2011 (14)	31 patients with ischemic stroke (12 = statin treatment prestroke, 19 = no statin treatment prestroke).	MRI within 4.5 and 6 hours poststroke. MRI before and during Gd injection. MTT = CBV/CBF. Measures of reperfusion (prolonged MTT; absolute reperfusion; relative reperfusion).	Greater reperfusion in patients using statins compared with untreated patients across MTT thresholds. Statin group had greater neurological improvement than untreated group. Statins have anti-inflammatory effects: by inhibition leukocyte and cytokine activation, they mitigate ischemia-reperfusion injury and may prevent no-reflow (i.e., tissue reperfusion not restored despite vessel recanalization).	0
Qiao *et al.*, 2012 (16)	47 patients referred for carotid plaque evaluation. 24 symptomatic (stroke/TIA), 23 nonsymptomatic.	MRI ≤12 weeks if symptomatic. MRI before and 5 min after Gd injection. Two raters identified neovascularity (adventitial enhancement) and IPH.	Neovascularity and IPH in carotid plaque are independently associated with previous cerebrovascular events, even when adjusted for statin use. Inflammation may further enhance adventitial enhancement but is not possible to isolate with this method.	0
Qiao *et al.*, 2014 (15)	27 patients with cerebrovascular ischemic events (20 acute stroke, 2 subacute stroke, 3 chronic stroke, 2 TIA).	MRI acute <4 weeks, subacute = 4−12 weeks, chronic >12 weeks. MRI before and 5 min after Gd injection. Plaque enhancement grades (0 = similar or less enhanced than intracranial arterial walls without plaque; 1 = greater than 0 but less than pituitary infundibulum; 2 = similar or greater than infundibulum).	Grade 2 associated with culprit plaque (only or most stenotic lesion upstream from stroke) when adjusted for plaque thickness. Grade 0 only in nonculprit plaques (not in vascular territory of stroke). Culprit plaques have higher degree of contrast enhancement than nonculprit plaques. Contrast enhancement of intracranial atherosclerotic plaque is associated with its likelihood to have caused an ischemic event. High degree of enhancement in intracranial plaques responsible for ischemic events likely reflects increased inflammatory activity.	0
Natori *et al.*, 2016 (17)	30 patients with acute noncardioembolic stroke in middle cerebral artery (M1) territory	MRI 3–27 days after stroke. MRI before and after Gd injection. CR: (signal intensity plaque/signal intensity corpus callosum) × 100 Contrast enhancement (CR postcontrast 1.2× > precontract).	In M1 plaques, CRs ipsilateral to infarct > contralateral, particularly in patients with lacunar infarcts. CRs in nonlacunar group higher than CRs in lacunar group. Substantial contrast enhancement of the plaques in 20% of the M1s. Plaque enhancement typically due to neuroinflammation.	0
Choi *et al.*, 2017 (18)	264 patients with acute ischemic stroke.	MRI within 7 days of symptom onset. MRI before and 5 min after Gd injection. BBB permeability (HARM).	67 patients HARM positive and 197 patients HARM negative. HARM-negative was associated with small vessel occlusion. HARM positive associated with embolic infarctions (large artery atherosclerosis, cardioembolism). HARM positive likely associated with BBB permeability resulting from inflammation.	0
Wardlaw *et al.*, 2017 (19)	201 patients with mild ischemic lacunar or cortical stroke.	MRI 1–3 mo after stroke. MRI before and after Gd injection sequentially 20 times for 24 min. BBB leakage (linear mixed modeling of signal enhancement slopes to identify tissue- and patient-specific differences).	BBB leakage and interstitial fluid higher in WMH than NAWM. BBB leakage in NAWM increased with proximity to WMH, WMH severity, age, hypertension. BBB leakage in WMH predicted declining cognition at 1 year. Systemic inflammation is common in SVD and might be involved in declining cognition.	0

Table 2. Continued

Study	Sample	Design and Analysis	Results and Conclusions	Validation
Arba *et al.*, 2017 (20)	212 patients with acute ischemic stroke.	MRI acute phase of ischemic stroke. MRI before and during Gd injection. SVD burden (points for lacunes, WMH, brain atrophy). BBB leakage (mean value of all voxels > derangement threshold within ischemic area and healthy tissue).	BBB leakage present in 175 and 205 patients in ischemic and nonischemic areas, respectively. Lacunar infarcts associated with BBB leakage in ischemic area. Brain atrophy associated with BBB leakage in ischemic and nonischemic areas. Increasing SVD grade associated with BBB leakage in ischemic and nonischemic areas. Neuroinflammation may worsen BBB function in SVD.	0
O'Connell *et al.*, 2017 (21)	27 patients with ischemic stroke.	MRI 24 hours after ED admission. MRI before and during Gd injection. BBB permeability (HARM). Peripheral blood to measure *AKAP7* expression levels.	*AKAP7* associated with BBB disruption. *AKAP7* predominantly expressed by lymphocytes in peripheral blood, which produce proinflammatory cytokines that mediate immune cells into brain. *AKAP7* expression levels may be biomarker for poststroke BBB complications, caused by invasive lymphocytes in peripheral blood.	2: increased BBB permeability (measured by Gd-enhanced MRI) correlated with heightened lymphocyte expression (measured by *AKAP7* expression in peripheral blood).
Gupta *et al.*, 2018 (22)	65 patients with acute ischemic stroke and WMH.	MRI acute phase of ischemic stroke. MRI before and during Gd injection. BBB leakage (% leak = fractional decrease in CBV due to Gd leakage).	Hypertension but no other vascular risk factors associated with BBB disruption. Nonhypertensive patients have more severe WMH in deep WM than periventricular region. WMH due to accumulation of lacunar infarcts and progressive brain injury from inflammation.	0
Nada-Reishvili *et al.*, 2018 (23)	33 patients that did not receive any reperfusion therapy during acute (<12 hours) ischemic stroke.	MRI at baseline, 24 hours, and 5 days. MRI before and during Gd injection. Baseline MRI compared with post-Gd at 24 hours. Baseline blood (monocyte count). BBB permeability (HARM).	HARM in 27% (HARM+). Baseline lesion volume larger in HARM+. Lesion growth in HARM+ at 24 hours. Increased monocytes in HARM+. Activated monocytes express higher levels of MMP-9, which might result in BBB disruption and appearance of HARM. Tissue damage through BBB likely by proinflammatory monocytes.	0
Rost *et al.*, 2018 (24)	184 patients with acute ischemic stroke.	MRI <9 hours after stroke. MRI before and during Gd injection. BBB leakage rates (K2 coefficients) in contralesional NAWM.	Higher K2 correlated with greater stroke severity and worse 90-day functional outcome. K2 associated with WMH volume and mean diffusivity in NAWM. Increased BBB permeability associated with loss of WM microstructure and worse poststroke outcomes.	0
Wu *et al.*, 2018 (25)	61 patients with unilateral anterior circulation ischemic stroke.	MRI <1 mo after stroke. MRI before and 5 min after Gd injection. Lesion enhancement grade (0 = plaque ER ≤ reference wall ER; 1 = reference wall ER < plaque ER < pituitary infundibulum ER; 2 = plaque ER ≥ pituitary infundibulum ER). Enhancement pattern (type 1 <50% cross-sectional wall involvement; type 2 ≥50% cross-sectional wall involvement).	Grade 2 contrast enhancement and type 2 enhancement pattern independently associated with culprit lesions (i.e., only lesion within vascular territory of stroke or most stenotic lesion when multiple plaques present within same vascular territory of stroke). High signal on CE-MRI, grade 2 contrast enhancement, and type 2 enhancement pattern associated with cerebrovascular ischemic events. Contrast enhancement is a marker of neovascularization and inflammation. Culprit lesions are likely to possess greater neovascularization and/or inflammation activities.	0

Table 2. Continued

Study	Sample	Design and Analysis	Results and Conclusions	Validation
Lublinsky *et al.*, 2019 (26)	124 patients with aneurysmal subarachnoid hemorrhage. PC patients (n = 78 abnormal tissue increased). NPC patients (n = 46 abnormal tissue decreased).	MRI 24–48 hours, 6–8 days, 12–15 days, and 6–12 mo after hemorrhage. MRI before and 5 min after Gd injection. BBBD—each enhanced voxel-assigned enhancement level normalized to 0–1 range.	Brain volume with BBBD larger in PC patients at 24–48 hours and persisted at all time points. Highest probability of BBBD voxel to become pathological at distance of ≤1 cm from brain with apparent pathology. BBBD at 24–48 hours predicts clinical outcome. BBBD in aneurysmal subarachnoid hemorrhage likely due to neuroinflammation and astroglial activation.	0
Neurological Disorders: TBI/Concussion				
Cho *et al.*, 2016 (28)	66 patients with TBI (33 young: 19–35 years; 33 old: 60–89 years).	MRI <48 hours after TBI. Second MRI 1 week (25 young and 23 old). MRI before and during Gd injection. MRI to confirm TBI. Microarray gene expression in peripheral blood.	75% of patients had TBI confirmed by MRI within 48 hours. At follow-up, positive MRI for TBI decreased in young patients to 32%, but not in old patients. Young patients had greater expression of inflammatory regulatory genes at both times. Older patients had reduced activity of growth factor gene. Older patients recover less well from TBI due to changed immune regulation and neurorecovery.	1: gene expression of inflammatory regulatory genes was measured from peripheral blood and found to be enhanced in younger patients. Gene activity was not statistically compared with MRI findings. Hence, direct validation is missing.
Livingston *et al.*, 2017 (29)	40 patients with TBI. 17 TMI+ patients. 23 TMI− patients.	MRI <48 hours after TBI. MRI before and during Gd injection. Microarray gene expression in peripheral blood.	76 genes differentially expressed in TMI+ compared with TMI−. 4 identified genes associated with initiating inflammatory mediators, phagocytosis, and other regulatory mechanisms were >1.5-fold higher in TMI+ patients relative to TMI− patients. Postcontrast MRI detects meningeal injury and has a unique biological signature observed through gene expression. Acute inflammatory response caused by injury to the meninges after a concussion.	2: patients with Gd-enhanced meninges exhibited increased peripheral expression of genes initiating inflammatory response compared with patients without Gd-enhanced meninges.
Neurological Disorders: Parkinson's Disease				
Ding *et al.*, 2021 (30)	398 patients with iPD. AP groups: 168 patients with MSA. 146 patients with PSP-RS. 11 patients with DLB. 5 patients with CBD. 23 patients with VP.	T1 black-blood scan before and after Gd administration to reconstruct 3D meningeal lymphatic vascular system. 2D T1 black-blood sequence DCE-MRI after Gd injection to evaluate mLVs flow. Animal immunohistochemical substudy: α-syn PFF injected into bilateral striatum of mice to generate a mouse model of PD.	Reduced flow through mLVs along superior sagittal sinus and sigmoid sinus and delayed deep cervical lymph node perfusion iPD vs. AP. No mLV size difference in iPD or AP vs. control subjects. α-syn PFF–treated mice exhibited emerging α-syn pathology, followed by delayed meningeal lymphatic drainage, loss of tight junctions in meningeal lymphatic endothelial cells, and increased inflammation of meninges. Blocking flow through mLVs in α-syn PFF–treated mice increased α-syn pathology and exacerbated motor and memory deficits. Meningeal lymphatic drainage dysfunction aggravates α-syn pathology and contributes to PD progression.	1: in an animal model of PD, PD pathology was associated with increased meningeal macrophages measured by immunofluorescent staining of meningeal tissue. While this provides indirect evidence that meningeal lymphatic dysfunction in PD is associated with inflammation, direct associations with Gd-enhanced measures of lymphatic flow are missing in humans and mice.

Table 2. Continued

Study	Sample	Design and Analysis	Results and Conclusions	Validation
Psychiatric Disorders: Depression				
Kallaur *et al.*, 2016 (31)	42 MSD+ patients. 108 MSD− patients. 249 HC subjects.	MRI before and after Gd injection. Gd-enhanced MRI (yes/no). Depression (depressive subscale—Hospital Anxiety & Depression Scale). Serum levels of proinflammatory cytokines (IL-1β and IL-6) and Th2 cytokines (IL-4 and IL-10) assayed.	Increased IL-6 and lower IL-4 and albumin levels MSD+ vs. MSD−. Increased IL-6 and lower albumin inflammatory depression markers. Lower IL-4 may indicate lowered negative immunoregulatory potential and elevated immune-inflammatory responses. Gd-enhancement negatively associated with depression. Low-grade inflammation, subtle BBB permeability, degeneration, and repair more likely accompanied by depression than acute inflammatory state.	1: Depression in patients with MS was associated with decreasing Gd enhancement and peripheral inflammation (increased IL-6, lower IL-4 and albumin). However, Gd enhancement and peripheral inflammation markers were not directly compared.

2D, two-dimensional; 3D, three-dimensional; -syn, α-synuclein; AP, atypical Parkinson's disease; BBB, blood-brain barrier; BBBD, blood-brain barrier dysfunction; CBD, corticobasal degeneration; CBF, cerebral blood flow; CBV, cerebral blood volume; CE-MRI, contrast-enhanced magnetic resonance imaging; CR, contrast ratio; DCE-MRI, dynamic contrast-enhanced MRI; DLB, dementia with Lewy bodies; ED, emergency department; ER, enhancement ratio; Gd, gadolinium; HARM, hyperintense acute reperfusion marker; HC, healthy control; IL, interleukin; iPD, idiopathic Parkinson's disease; IPH, intraplaque hemorrhage; mLV, meningeal lymphatic vessel; MPD, mean permeability derangement; MRI, magnetic resonance imaging; MS, multiple sclerosis; MSA, multiple systems atrophy; MSD+, MS with depression; MSD−, MS without depression; MTT, mean transit time; NAWM, normal-appearing white matter; NPC, nonprogressive course; PC, progressive course; PD, Parkinson's disease; PFF, preformed fibril; PSP-RS, progressive supranuclear palsy-Richardson syndrome; SVD, small vessel disease; TIA, transient ischemic attack; TBI, traumatic brain injury; Th, T helper type; TMI, traumatic meningeal injury; TMI+, TMI with abnormal enhancement of meninges; TMI−, TMI without abnormal enhancement of meninges; VP, vascular parkinsonism; WM, white matter; WMH, white matter hyperintensity.

MRI cannot detect subtle inflammation occurring with minimal BBB disruption. Black-blood imaging is a relatively novel vascular imaging strategy that offers some advantages over bright-blood techniques: owing to the suppression of intraluminal signal, vessels do not generate pulsation artifacts and can be more clearly delineated in Gd-enhanced sequences. It enables imaging of inflammation localized to blood vessels and can be applied to plaque enhancement in intracranial atherosclerosis, therefore offering an improved technique to image neuroinflammation across neurological disorders.

Ultrasmall Superparamagnetic Particles of Iron Oxide–Based CE-MRI. Our database search identified two studies using ultrasmall superparamagnetic particles of iron oxide (USPIO)–based CE-MRI to study neuroinflammation. Both studies used ferumoxytol. One of the studies was conducted in patients with minor ischemic stroke (small vessel disease) (see Table 3) (32). The study observed intravascular uptake of USPIOs but did not find any evidence for parenchymal uptake. This was interpreted to reflect a lack of inflammatory cells and BBB leakage in patients with small vessel disease, where neuroinflammation is expected to be subtle and diffuse. The authors suggested that USPIO uptake in the parenchyma may only be visible in disorders with a more extensive inflammatory component. The second study used USPIO-enhanced MRI to test whether macrophage-mediated inflammation of cerebral artery walls and brain parenchyma was associated with migraine pathophysiology (33). Migraine attacks were not associated with increased USPIO uptake on the pain side of the brain compared with the nonpain side. The study included a preclinical component, which confirmed that USPIO-enhanced MRI detects macrophage-mediated neuroinflammation. The main findings were therefore interpreted to indicate that macrophage-mediated neuroinflammation was not associated with migraine without aura.

The lack of studies using USPIO-enhanced MRI to investigate neuroinflammation is likely due to its relative novelty and availability. Preliminary findings and advancements of USPIO-based CE-MRI make it a promising imaging modality to study neuroinflammation. An attractive feature is that it seems to be tightly linked to macrophage infiltration, which is an important process of the neuroinflammatory cascade. Compared with Gd, USPIOs can cross the intact BBB. This offers the advantage of making it applicable to less severe expressions of neuroinflammation associated with the majority of neurological and psychiatric disorders.

MRI Markers Sensitive to Water Content and Tissue Compartments

Diffusion Kurtosis Imaging. Diffusion kurtosis imaging (DKI) has been used to study neuroinflammation in mild TBI (34), Alzheimer's disease (35,36), and schizophrenia spectrum disorder (37) (Table 4). All studies reported altered kurtosis metrics in patient groups relative to healthy control subjects. However, while these findings were interpreted to reflect possible inflammatory processes, they were not assessed in the context of other measures of inflammation. In a concurrent positron emission tomography (PET)–MR study, Dong *et al.* (36) reported that amyloid-beta (Aβ) burden was associated with both changed kurtosis and diffusion metrics (38). Increased diffusion hindrance was interpreted to reflect inflammation that accompanies rising Aβ burden. However,

Table 3. Studies in Neurological Disorders Using USPIO-Based CE-MRI to Study Neuroinflammation

Study	Sample	Design and Analysis	Results and Conclusions	Validation
Stroke				
Thrippleton *et al.*, 2019 (32)	12 patients with cerebral SVD.	MRI >1 mo after minor ischemic stroke. MRI before and immediately, 24–30 h, and 1 mo after USPIO infusion. Absolute and blood-normalized relaxometry (R_1 and R_2*) in WM and deep GM, WMH, and lesions.	Increased relaxation rate (R_1 and R_2*) in all tissues immediately and 24–30 h after USPIO. R_2* returned to baseline at 1 mo. Narrower distributions for R_2*. MRI relaxometry allows to quantify USPIO uptake. R_2* is more sensitive to USPIO than R_1. USPIO is eliminated after 1 mo. No association with inflammatory cells or BBB leakage.	0
Migraine				
Khan *et al.*, 2019 (33)	28 patients with migraine without aura. 4 HC subjects.	MRI >5 days since last migraine. Patients: baseline MRI, followed by 200 mg cilostazol to trigger migraine. 12 patients received 6 mg sumatriptan to treat migraine. All participants underwent MRI >24 h after USPIO infusion. Changes in relaxation rates (ΔR2*/ ΔR1) after USPIO minus baseline in thalamus, pons, ACA, MCA, and PCA territories between pain side and nonpain side.	No difference in USPIO uptake comparing pain and nonpain side in patients with migraine. Greater increase in R2* in patients who did not receive sumatriptan compared with those who did receive sumatriptan in ACA territory. Within ACA territory, ΔR2* was larger in pain side of patients who were not treated with sumatriptan. Unilateral attacks of migraine without aura are not associated with unilateral macrophage-mediated inflammation. Sumatriptan alleviates migraine by a mechanism independent of hindering inflammation.	4—capsaicin injections were placed subcutaneously in the trigeminal nerve area of mice to induce inflammation. Bioluminescence imaging using the macrophage marker lucigenin confirmed macrophage presence coinciding within the USPIO-enhanced site.

ACA, anterior cerebral artery; BBB, blood-brain barrier; CE-MRI, contrast-enhanced magnetic resonance imaging; GM, gray matter; HC, healthy control; MCA, middle cerebral artery; MRI, magnetic resonance imaging; PCA, posterior cerebral artery; SVD, small vessel disease; USPIO, ultrasmall superparamagnetic particles of iron oxide; WM, white matter; WMH, white matter hyperintensity.

while neuroinflammation and Aβ increase during prodromal stages of Alzheimer's disease, cortical inflammation has repeatedly been found to decrease with progression from prodromal to clinical manifestation of Alzheimer's disease, despite a continual increase in Aβ (38). Amyloid deposition is therefore not directly indicative of inflammation. Hence, while DKI may under certain circumstances be associated with inflammatory processes, it does not explicitly model neuroinflammation.

Free-Water Imaging. Free-water (FW) imaging (see Figure 3) has been used to study neuroinflammation across several disorders, including stroke (39–41), TBI (42), Alzheimer's disease (43–49), and Parkinson's disease (50–53) (Table 5). In Alzheimer's disease, increased FW has been linked to elevated tau (43), Aβ (48) measured from blood and cerebrospinal fluid (CSF), and global amyloid PET values in the brain (46). These associations were particularly strong in the hippocampus, where intraneuronal tau, which is associated with inflammatory reactions and neuronal atrophy, accumulates from midlife (54). Postmortem findings have reported that some individuals can tolerate large amounts of tau accumulation and Aβ deposition without experiencing dementia. Of note, these individuals exhibited substantially lower glial activation typically observed in Alzheimer's pathology, indicating that Aβ and tau pathologies with simultaneous glial activation may reflect a mediator for neurotoxicity and cognitive decline (55). Collectively, these findings provide strong support for FW as a proxy of an inflammatory process, namely glia activation, in Alzheimer's disease. Several studies in Parkinson's disease reported increased FW in the substantia nigra. While some studies suggest that this may reflect dopaminergic neuron depletion, the presence of Lewy bodies and Lewy neurites, and contraction of the neuropil (56), others speculate that it is due to neuroinflammation (50,52). All of these features are commonly observed in Parkinson's disease. In the absence of histopathological evidence, it is impossible to discern whether increased FW is caused by one or several of these pathologies. Finally, a study by Pasternak *et al.* (42) investigated hockey players before and after concussion and observed decreased FW in regions overlapping with decreased radial and axial diffusivity. Reduced radial diffusivity typically denotes increased myelin content. In the context of decreased FW, however, it may point to axonal swelling, which occurs as part of the immune response in the acute and subacute stages of concussion (57). Concurrent reduction of FW and axial

Table 4. Studies in Neurological and Psychiatric Disorders Using DKI to Study Neuroinflammation

Study	Sample	Design and Analysis	Results and Conclusions	Validation
Neurological Disorders: TBI/Concussion				
Grossman *et al.*, 2013 (34)	20 patients with mTBI. 16 HC subjects.	TBSS and ROI analysis in thalamus (MK, FA, MD, CBF). Neuropsychological battery (attention, concentration, executive functioning, memory, learning, information processing).	Baseline mTBI vs. HC: lower MK, FA, and CBF; higher MD in thalamus, internal and external capsule, CC, cingulum, optic radiation, total deep GM, and total WM. Follow-up mTBI vs. HC: lower MK and CBF and higher MD in thalamus, CC, cingulum, optic radiation, total deep GM, and total WM. mTBI: higher FA and lower MD between baseline and follow-up. Cognitively impaired vs. unimpaired mTBI had lower MK in thalamus. MK results suggest inflammation marked by reactive astrogliosis.	0
Neurological Disorders: Alzheimer's Disease				
Fieremans *et al.*, 2013 (35)	12 patients with MCI. 14 patients with AD. 15 age-matched HC subjects.	TBSS and ROI analysis of CC (AWF, D_{axon}, $D_{e,\parallel}$, $D_{e,\perp}$).	Increased $D_{e,\parallel}$ and $D_{e,\perp}$ in several WM tracts in HC vs. MCI and MCI vs. AD; decreased AWF in MCI vs. AD, particularly in CC. Extra-axonal diffusivity ($D_{e,\perp}$, $D_{e,\parallel}$) differences between HC and MCI suggests pathological changes such as astrocytosis or inflammation.	0
Dong *et al.*, 2021 (36)	21 patients with MCI or early Alzheimer's disease. 23 age- and gender-matched HC subjects. 3 groups based on Aβ burden: Aβ− (mSUVr ≤ 1.00), Aβi (1.00 < mSUVr <1.17), Aβ+ (mSUVr ≥ 1.17).	PET-MRI. TBSS (FA, RD, RK, AWF). GM volumes. WM lesion volume from automatic segmentation. Florbetapir SUVs averaged across anterior and posterior cingulate, medial orbitofrontal lobe, parietal lobe, and medial temporal lobe.	Aβi: more restricted diffusion (higher FA, RK, and AWF; lower RD) than both Aβ− and Aβ+ in genu of CC, anterior corona radiata, and fornix. FA, RK, and AWF correlated with SUV in the Aβ−/Aβi cohort and negatively in the Aβi/Aβ+ cohort; opposite pattern for RD. Transient period of increased diffusion restriction may be due to inflammation that accompanies rising Aβ burden.	0
Psychiatric Disorders: Schizophrenia				
McKenna *et al.*, 2019 (37)	18 patients with SZ spectrum disorder. 19 HC subjects.	T2, T1, multishell DWI. 68 FreeSurfer cortical GM parcellations and 4 cortical lobes (MD, MK, area, and thickness).	Increased MK and MD in SZ vs. HC in temporal lobe, fusiform, inferior temporal, middle temporal and temporal pole, and PCC. Increased kurtosis may reflect higher-order inflammation.	0

Aβ, beta amyloid; Aβ−, low Aβ; Aβi, intermediate Aβ; Aβ+, high Aβ; AWF, axonal water fraction; CBF, cerebral blood flow; CC, corpus callosum; D_{axon}, intrinsic diffusivity inside axons; $D_{e,\parallel}$, extra-axonal axial diffusivity; $D_{e,\perp}$, extra-axonal radial diffusivity; DKI, diffusion kurtosis imaging; DWI, diffusion weighted imaging; FA, fractional anisotropy; GM, gray matter; HC, healthy control; MCI, mild cognitive impairment; MD, mean diffusivity; MK, mean kurtosis; MRI, magnetic resonance imaging; mSUVr, mean standardized uptake value ratio; mTBI, mild traumatic brain injury; PCC, posterior cingulate cortex; PET, positron emission tomography; RD, radial diffusivity; RK, radial kurtosis; ROI, region of interest; SUV, standardized uptake value; SZ, schizophrenia; TBI, traumatic brain injury; TBSS, tract-based spatial statistics; WM, white matter.

diffusivity are likely to reflect an increase in the number and size of glia cells (57). This is because accumulation and augmentation of glia cells would lead to a general isotropic reduction of the extracellular space (i.e., decrease FW) and because diffusivity within glia cells is more restricted than along axons, axial diffusivity is expected to decrease simultaneously. While plausible, these interpretations need to be considered cautiously until corroborated by other methods.

In psychiatric disorders, FW imaging has been used to study major depressive disorder (58), bipolar disorder (59), and schizophrenia (60–67) (Table 5). A small study in 17 female patients with major depressive disorder found increased FW-corrected fractional anisotropy and axial diffusivity (but not radial diffusivity or FW) (58). Contrary to this finding, a recent study in post-stroke depression reported increased FW in the reward system to be associated with depression severity in stroke survivors (41). Given the accumulating evidence for a role of inflammation in depression (68), further FW investigations in larger, more diverse depression samples supplemented with inflammation markers derived from blood or CSF are required before ultimate conclusions as to the usefulness of FW imaging to detect neuroinflammatory processes in depressive disorders can be drawn.

Several studies found evidence for increased extracellular FW in the absence of large-scale microstructural changes in patients with first-episode schizophrenia (Figure 4) (60,64),

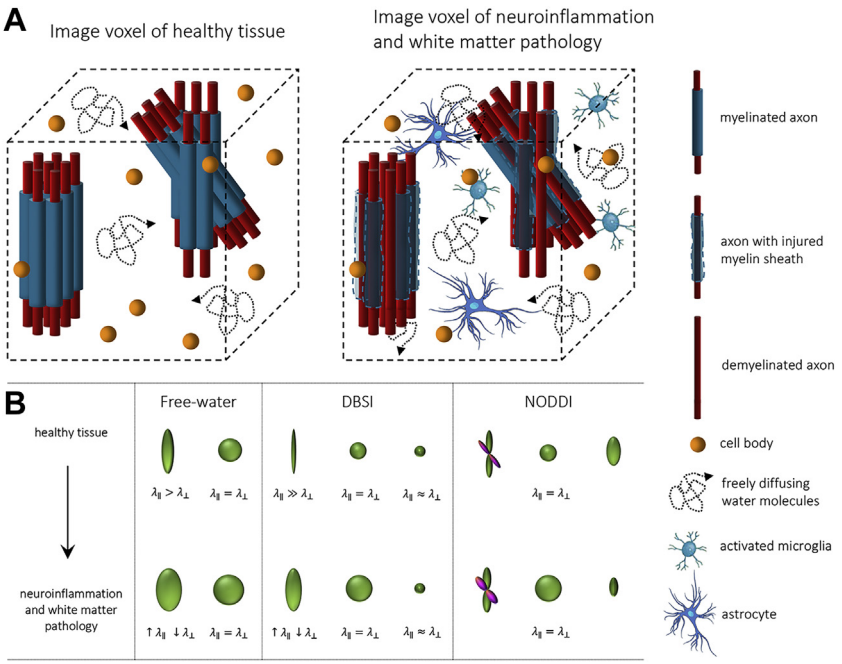

Figure 3. Comparison of diffusion magnetic resonance imaging models to estimate aspects of neuroinflammation. **(A)** Schema of image voxels with healthy tissue (left) and neuroinflammation and white matter pathology (right). **(B)** Diffusion models for free-water imaging, DBSI, and NODDI. The upper panel shows the diffusion models in a healthy tissue environment (corresponding to image voxel of healthy tissue), and the lower panel demonstrates how these models change in inflamed and insured tissue environments (corresponding to image voxel of neuroinflammation and white matter pathology). Free-water imaging is a two-compartment model: an isotropic tensor is used to estimate the amount of freely diffusing water molecules within a voxel, and a second tensor represents the average anisotropic diffusion across the voxel. DBSI estimates multiple anisotropic diffusion tensors to model neuronal architecture within a voxel and a spectrum of isotropic diffusion tensors, representing cellular and subcellular structures, as well as free-water. NODDI considers diffusion within three compartments: restricted diffusion in the intraneuronal compartment (i.e., water molecules are mainly limited to diffuse along axons), hindered diffusion in the extracellular compartment (i.e., water molecules are not limited to diffuse in one direction but are confined in their movement by other cell bodies), and free, isotropic diffusion. $\lambda_{\parallel}$ = parallel diffusion; $\lambda_{\perp}$ = perpendicular diffusion. DBSI, diffusion basis spectrum imaging; NODDI, neurite orientation dispersion and density imaging.

with the reverse pattern reported in chronic schizophrenia (61,62,66). This is consistent with the view that the early stages of schizophrenia are marked by neuroinflammation rather than substantial changes in underlying neuronal architecture, which manifest in later illness stages (60). Similarly, in bipolar disorder, increased FW was associated with recent psychiatric episodes, which may imply a shared pathology with schizophrenia (59). Furthermore, while microstructural changes in the cingulum bundle were reported to be associated with state and trait delusion in schizophrenia, increased FW was linked only to state delusions (63), indicating a link between neuroinflammation and active psychotic episodes. A recent study found that higher peripheral proinflammatory signaling of interleukin 6 and tumor necrosis factor α was associated with widespread increased brain FW in patients with schizophrenia but not in healthy control subjects (65). These findings substantiate previous reports of cytokine dysregulation and FW abnormalities in schizophrenia and demonstrate a direct relationship between peripheral inflammation and FW (Table 5).

The critical limitation of FW imaging is that it is unable to discriminate inflammation from ex vacuo increases due to atrophy. Increases in extracellular FW have also been attributed to elevated tau and amyloid, accumulation of Lewy bodies and neurites, neuron depletion, and axonal swelling, complicating the interpretability of this novel measure. However, these processes are typically accompanied by inflammation, which may be the underlying mechanism leading to observed FW changes. Recent efforts to validate FW as an imaging proxy of neuroinflammation in preclinical models (69) and the complementation of FW imaging with peripheral markers of inflammation (65) are promising first steps toward establishing the validity of this method.

Neurite Orientation Dispersion and Density Imaging. Identified neurite orientation dispersion and density imaging (NODDI) studies investigating neuroinflammation were limited to TBI (70,71), Alzheimer's disease risk states (72), schizophrenia (73), and depressive symptom development in response to interferon alpha treatment (74) (Table 6). In line with preclinical findings, increased orientation dispersion index was observed in concussed athletes with higher symptom burden and a longer recovery time (70) as well as unmedicated and antipsychotic-naïve patients with schizophrenia (73). Contrary to these findings, a study by Metzler-Baddeley *et al.* (72) did not find a link between NODDI measures and systemic inflammation or obesity-related effects on limbic white matter microstructure, which is commonly involved in late-onset Alzheimer's disease. A study by Dowell *et al.* (74) investigated depressive symptoms as a result of interferon alpha treatment in patients with hepatitis C. Interferon alpha promotes antiviral immune responses and is able to cross the BBB. While fatigue linked with treatment was found to be associated with neurite density index, a NODDI metric thought to be sensitive to astrocytic processes, no associations were observed with orientation dispersion index or depressive symptoms.

Two studies (70,72) investigated the extracellular FW component derived from NODDI, which measures random motion of water molecules in the extracellular space and should, therefore, exhibit the closest resemblance to the FW component derived from FW imaging. However, no changes in FW were observed in concussed athletes (70) or individuals at risk for Alzheimer's disease (72). While this might seem contradictory, by differentiating more subvoxel compartments than FW imaging, NODDI may provide more detailed

Table 5. Studies in Neurological and Psychiatric Disorders Using FW Imaging to Study Neuroinflammation

Study	Sample	Design and Analysis	Results and Conclusions	Validation
Neurological Disorders: Stroke				
Archer *et al.*, 2017 (39)	23 patients with ischemic stroke with affected function in contralateral hand 6 mo prior. 23 age-matched HC subjects.	MRI > 6 mo (mean = 7.8 years). Tract templates from probabilistic tractography of PMd-CST and M1-CST (FA_T, FW).	Increased FW in stroke patients in large portions of M1-CST and PMd-CST in lesioned hemisphere. FW in cortical regions strongest predictor of grip strength in stroke. Increases in FW in cortical regions may reflect neuroinflammation and/or reduced cellular density.	0
Duering *et al.*, 2019 (40)	57 patients with genetically defined SVD (CADASIL). 444 patients with sporadic SVD. 28 HC subjects.	TBSS (MD, FA, MD_T, FA_T, FW). Neuropsychological testing (processing speed, disability).	CADASIL vs. HC: lower FA and increased MD and FW overlap. Diffusion alterations in CADASIL and sporadic SVD mostly driven by increased FW. FW strongest association with processing speed. Increased FW may indicate disruption of BBB.	0
Oestreich *et al.*, 2020 (41)	12 stroke patients with PSD. 34 stroke patients free of PSD. 16 HC subjects.	Connectome analyses with FA_T-/FW-weighted matrices. Tractography of cingulum subregions and medial forebrain bundle (FA_T/FW). GM volume from reward structures.	Subnetworks of decreased FA_T-weighted and increased FW-weighted connectivity PSD vs. HC mapped onto reward system. FA_T, FW, and GM volume in reward structures predicted PSD severity. FW in reward system may be indicative of inflammatory processes contributing to the development of PSD.	0
Neurological Disorders: TBI/Concussion				
Pasternak *et al.*, 2014 (42)	7 patients with concussion.	MRI before and after concussion. TBSS (FW, FA_T, AD_T, RD_T).	Pre- vs. postconcussion: FA increased; FA_T same; FW, AD_T, and RD_T decreased. Decreased RD_T and FW might indicate axonal swelling. Decreased AD_T and FW might indicate increased glial cells due to neuroinflammation.	0
Neurological Disorders: Alzheimer's Disease				
Hoy *et al.*, 2017 (43)	70 participants without dementia: positive or negative for parental history of Alzheimer's disease.	Deterministic tractography of fornix, superior cingulum bundle, and five subdivisions of CC (FA, MD, FW, FA_T, MD_T). CSF (Alzheimer's disease pathology).	Alzheimer's disease pathology (CSF) associated with altered microstructure on both DTI and DTI_T metrics. Elevated p-tau/Aβ and t-tau/Aβ ratios associated with higher FW in frontal and temporal lobe WM. Uncorrected association between MD and YKL-40 (microglial activity) indicates inflammation.	3: ratio of YKL-40 to $Aβ_{42}$ (suggested to reflect inflammation) showed positive association with FW. YKL-40 association with MD was interpreted as increasing neuronal cell vulnerability due to inflammation.
Ji *et al.*, 2017 (44)	41 patients with Alzheimer's disease without concomitant CeVD (AD − CeVD). 25 patients with Alzheimer's disease with CeVD (AD + CeVD). 19 patients with VD. 30 HC subjects.	TBSS (FA, RD, AD, FW, FA_T, AD_T, RD_T). Dementia severity (Clinical Dementia Rating Sum of Boxes scores). General cognitive performance (Mini-Mental State Examination scores).	FW: AD + CeVD/VD > AD − CeVD/HC in WMH and AD + CeVD/VD/AD − CeVD > HC in NAWM. Correlation between FW (averaged across skeleton) and dementia severity across all patients. Increased FW in NAWM in AD − CeVD suggests neuroinflammation related BBB permeability and microvascular degeneration.	0
Montal *et al.*, 2017 (45)	41 patients with MCI. 31 patients with Alzheimer's disease. 254 HC subjects (Aging-Alzheimer's Association stages: stage 0, 220; stage 1, 25; stage 2/3, 9).	CSF (enzyme-linked immunosorbent assay). Surface-based DTI (MD, FW). T1 (CTh).	Stage 1 vs. 0: increased CTh, lower MD and FW. Stage 2/3/MCI/Alzheimer's disease vs. 0: reduced CTh and higher MD and FW worsening with illness stage. Increased CTh and decreased MD/FW in asymptomatic Alzheimer's disease may be caused by amyloid-induced inflammatory response.	0

Table 5. Continued

Study	Sample	Design and Analysis	Results and Conclusions	Validation
Ofori *et al.*, 2019 (46)	58 elderly HC subjects. 78 patients with EMCI. 48 patients with LMCI. 54 patients with Alzheimer's disease.	Volume and FW of the hippocampus. Signal uptake value ratios for amyloid PET in the frontal lobe, anterior cingulate, precuneus, and parietal cortex relative to cerebellum. Genotyping for APOE ε2, ε3, ε4 alleles. $A\beta_{1-42}$, t-tau, and p-tau_{181} from CSF.	Increased hippocampal FW in EMCI vs. HC. No hippocampal volume differences. Hippocampal FW associated with low CSF $A\beta_{1-42}$ levels and high global amyloid PET values. Postmortem studies show intraneuronal tau accumulation in hippocampus from midlife, which is associated with inflammatory reactions and neuronal atrophy. This may explain observed FW increase in hippocampus.	0: while CSF and PET amyloid were associated with FW values, amyloid is an abnormal protein, not an inflammation marker and hence does not provide direct evidence for a link to inflammation.
Archer *et al.*, 2019 (47)	Two cohorts: 30 patients with Alzheimer's disease; 32 matched HC subjects. 26 patients with PSP; 31 matched HC subjects.	Probabilistic tractography in 100 HC subjects to create TCATT. FA_T and FW group differences in TCATT in patient cohorts.	Widespread increases in TCATT FW in Alzheimer's disease vs. HC; no FA_T changes. Widespread reduced FA_T and increased FW in TCATT in PSP vs. HC. Neuroinflammation or atrophy in commissural WM may be indicative of Alzheimer's disease and PSP.	0
Vipin *et al.*, 2019 (48)	21 Aβ-positive and 51 Aβ-negative cognitively normal elderly participants.	Hippocampal, GM, and WM volumes extracted using FreeSurfer recon-all segmentation. 18 WM tracts reconstructed with TRACULA.	Aβ-positive: increased uncinate fasciculus FW associated with worse Alzheimer's disease assessment scale scores. Aβ-positive: faster FA_T decrease in uncinate fasciculus and faster age-dependent right ILF FW increases. Right ILF FW increases associated with greater memory decline. Same results after controlling for GM, WM, and hippocampal volume. Aβ in brain activates inflammatory cascade, which may lead to greater extracellular water.	0
Ji *et al.*, 2019 (49)	54 patients with aMCI. 46 patients with Alzheimer's disease. 51 HC subjects.	TBSS (FA_T, FW). DMN FC using seed-based approach. Sparse varying coefficient model to investigate how the associations between abnormal brain measures and memory impairment varied throughout Alzheimer's disease continuum.	Lower FC in DMN related to worse memory in Alzheimer's disease continuum. Higher FW and lower FA_T in fornix showed stronger association with memory impairment in early aMCI stage; WM-memory associations decreased with increased dementia severity. Widespread small vascular degeneration and/or chronic neuroinflammation might play roles in memory deficit during early stages of Alzheimer's disease.	0
Neurological Disorders: Parkinson's Disease				
Ofori *et al.*, 2015 (50)	Single-site study: 28 patients with PD. 20 HC subjects. Multisite study: 78 patients with PD. 56 HC subjects.	ROIs in anterior and posterior SN (FW, FA_T, MD_T). SPECT imaging (SBR).	FW increased in posterior SN in PD vs. HC in both studies. Negative correlation between contralateral posterior SN FW and contralateral putamen SBR across groups in single-site study. Increased FW may be related to neuroinflammation.	0
Ofori *et al.*, 2017 (51)	184 patients with PD. 63 patients with MSA. 71 patients with PSP. 107 HC subjects.	ROIs in anterior and posterior SN (single tensor FA, MD, bitensor FW, FA_T, MD_T).	FW: posterior SN: PSP > MSA/PD > HC; anterior SN PSP > HC/ PD/FA_T: posterior SN: PSP > PD/HC; anterior SN: PSP > PD/HC/FA: posterior SN: PSP/MSA < HC; anterior SN: PSP < HC. Single-tensor FA may be reduced because of inflammation.	0

Table 5. Continued

Study	Sample	Design and Analysis	Results and Conclusions	Validation
Guttuso *et al.*, 2018 (52)	19 patients with PD. 19 age-matched HC subjects.	2 MRI (baseline, 3 years). ROIs in anterior and posterior SN (FW, FA, MD, AD, RD, FA_T, MD_T, AD_T, RD_T).	Increased baseline FW in anterior and posterior SN in PD vs. HC. Increased FW in anterior SN after 3 years in PD vs. HC. Increased FW may reflect tissue atrophy and inflammation, which are common in SN of patients with PD.	0
Andica *et al.*, 2019 (53)	20 patients with PD. 20 age- and gender-matched HC subjects.	TBSS and GBSS (FA, MD, AD, RD, FA_T, MD_T, AD_T, RD_T, FW).	TBSS: PD vs. HC: lower FA and FA_T and higher MD, MD_T, AD, AD_T, RD, RD_T, and FW. Reduced FA_T and increased MD_T/AD_T in anterior WM, increased FW in the posterior WM. GBSS: higher MD_T, AD_T, and FW. Neuroinflammation precedes neuronal degeneration in PD, whereas WM microstructural alterations precede changes in GM.	0
Psychiatric Disorders: Major Depressive Disorder				
Bergamino *et al.*, 2016 (58)	17 female patients with MDD. 18 female HC subjects.	TBSS (FA, RD, AD, FW, FA_T, AD_T, RD_T). Measures of stress (Perceived Stress Scale, Panic Disorder Severity Scale, Penn State Worry Questionnaire).	Decreased FA_T and AD_T in left IFOF in MDD vs. HC. Increased stress correlated with decreased IFOF AD_T in MDD. No differences in FW indicates that differences are likely not due to regional atrophy or neuroinflammation in MDD.	0
Psychiatric Disorders: Bipolar Disorder				
Tuozzo *et al.*, 2018 (59)	17 patients with chronic BD. 28 HC subjects.	TBSS (FA, FW, FA_T).	Lower FA in BD vs. HC in areas that overlapped with FW increases. FW increase could be indication of recent psychotic episodes. Neuroinflammation indicated by FW might be a shared pathology between chronic BD and early SZ.	0
Psychiatric Disorders: Schizophrenia/Psychosis				
Pasternak *et al.*, 2012 (60)	18 patients with FEP. 20 matched HC subjects.	TBSS (FA, MD, FW, FA_T).	FEP vs. HC: increased FW in WM and GM (41% left, 38% right), lower FA (31% left and right) and FA_T (1.25% left, 1.65% right), higher MD (54% left, 49% right). Neuroinflammation more prominent than WM degeneration in early stages of SZ.	0
Psychiatric Disorders: Schizophrenia				
Pasternak *et al.*, 2015 (61)	29 patients with chronic SZ. 25 matched HC subjects.	TBSS (FW, FA_T).	SZ vs. HC: increased FW (2.7% left, none right), decreased FA_T (4.3% left, 2.1% right). Limited FW increase in chronic SZ suggests less neuroinflammatory response relative to FEP. Greater FA reductions in chronic SZ vs. FEP, suggests WM degeneration with illness progression.	0
Oestreich *et al.*, 2016 (63)	34 patients with SZ with present-state delusions. 35 patients with SZ with remitted delusions. 17 patients with SZ with no history of delusions. 28 matched HC subjects.	Deterministic tractography of cingulum bundle, uncinate fasciculus, and fornix (FA_T, FW, AD_T, RD_T).	SZ + delusions vs. HC: reduced FA_T in cingulum; remitted SZ vs. HC: reduced FA_T right cingulum. SZ + delusions/remitted vs. HC: increased RD_t in cingulum. SZ + delusions vs. HC: increased FW in left cingulum. State and trait delusions in SZ are associated with microstructural processes and state delusions with neuroinflammation in cingulum.	0

Table 5. Continued

Study	Sample	Design and Analysis	Results and Conclusions	Validation
Oestreich *et al.*, 2017 (62)	281 patients with chronic SZ. 188 HC subjects.	ENIGMA-TBSS (FW, FA_T).	Reduced FA_T in SZ in anterior limb of internal capsule, posterior thalamic radiation, genu (CC), no increased FW after correction for multiple comparisons. Chronic SZ less marked by neuroinflammation than WM degeneration.	0
Lyall *et al.*, 2018 (64)	63 patients with FEP. 70 matched HC subjects.	TBSS (FA, FW, FA_T). Cognitive testing (MATRICS Consensus Cognitive Battery at baseline and after 12 weeks of antipsychotic treatment).	Lower FA across whole brain in FEP vs. HC overlapped with FW increase; limited FA_T decrease. Higher FW correlated with better neurocognitive functioning at 12 weeks of antipsychotic treatment. Increased FW during FEP may indicate acute neuroinflammatory process and/or cerebral edema and predict better functional outcome.	0
Di Biase *et al.*, 2020 (65)	497 patients with chronic SZ. 646 HC subjects.	8 cytokines (IFN-γ, IL-10, IL-12 [p70], IL-1β, IL-2, IL-6, IL-8, TNF-α). ENIGMA-TBSS (FA, FW, FA_T) in 199 SZ and 109 HC subjects.	Deregulation of cytokine levels in SZ evidenced by SZ > HC: IL-6, IL-8, TNF-α; SZ < HC: IL-2, IL-12. Higher proinflammatory signaling of IL-6 and TNF-α associated with higher FW levels in WM. Increased serum cytokines and FW in SZ in most major fibers; in HC subjects, relationship was limited to anterior CC and thalamic radiations. No relationship between cytokine levels and FA or FA_T. Inflammation is a putative mechanism underlying increases in brain FW levels in SZ.	2: peripheral cytokine levels were correlated with FW. Higher proinflammatory cytokines IL-6 and TNF-α were associated with widespread increasing FW, supporting FW as a marker of neuroinflammation.
Kragulkac *et al.*, 2019 (66)	42 patients with SZ (30 antipsychotic naïve, 12 untreated). 42 matched HC subjects.	MRI before and after a 6-week trial of risperidone. Whole-brain voxelwise analysis with FW and ODI.	Unmedicated and antipsychotic-naïve patients with SZ increased ODI in posterior limb of the internal capsule. No group differences in voxelwise FW or whole-brain ODI. 6.3% increase in whole-brain FW in unmedicated SZ vs. HC subjects. No changes after risperidone treatment. Increased ODI interpreted as lesser fiber uniformity in this area. Increased FW may reflect dynamic imbalance of inflammatory pathways across SZ illness stages.	0
Psychiatric Disorders: Clinically High Risk for Psychosis				
Tang *et al.*, 2019 (67)	50 CHR patients (40 never medicated). 50 age-, gender-, and parental socioeconomic status–matched HC subjects.	TBSS (FW, FA_T, RD_T, AD_T).	FA_T: CHR < HC; no FW differences. Lower FA_T in CHR associated with declined global functioning. Cellular but not extracellular alterations characterize CHR.	0

Aβ, amyloid beta; AD, axial diffusivity; AD_T, free-water corrected AD; aMCI, amnestic mild cognitive impairment; APOE, apolipoprotein E; BBB, blood-brain barrier; BD, bipolar disorder; CADASIL, cerebral autosomal dominant arteriopathy with subcortical infarcts and leucoencephalopathy; CC, corpus callosum; CeVD, cerebrovascular disease; CHR, clinically high risk for psychosis; CSF, cerebrospinal fluid; CTh, cortical thickness; DMN, default mode network; DTI, diffusion tensor imaging; DTI_T, free-water–corrected diffusion tensor imaging; EMCI, early mild cognitive impairment; ENIGMA, Enhancing Neuro Imaging Genetics Through Meta Analysis; FA, fractional anisotropy; FA_T, free-water–corrected fractional anisotropy; FC, functional connectivity; FEP, first-episode psychosis; FW, free-water; GBSS, gray matter–based spatial statistics; GM, gray matter; HC, healthy control; IFN-γ, interferon gamma; IFOF, inferior fronto-occipital fasciculus; IL, interleukin; ILF, inferior longitudinal fasciculus; LMCI, late mild cognitive impairment; M1-CST, primary motor corticospinal tract; MCI, mild cognitive impairment; MD, mean diffusivity; MD_T, free-water–corrected mean diffusivity; MDD, major depressive disorder; MRI, magnetic resonance imaging; MSA, multiple systems atrophy; NAWM, normal-appearing white matter; ODI, orientation dispersion index; PD, Parkinson's disease; PET, positron emission tomography; PMd-CST, dorsal premotor corticospinal tract; PSD, poststroke depression; PSP, progressive supranuclear palsy; p-tau, phosphorylated tau; RD, radial diffusivity; RD_T, free-water corrected RD; ROI, region of interest; SBR, striatal binding ratio; SN, substantia nigra; SPECT, single-photon emission computed tomography; SVD, small vessel disease; SZ, schizophrenia; TBI, traumatic brain injury; TBSS, tract-based spatial statistics; TCATT, trancallosal tract template; TNF-α, tumor necrosis factor α; TRACULA, TRActs Constrained by UnderLying Anatomy; t-tau, total tau; VD, vascular dementia; WM, white matter; WMH, white matter hyperintensity.

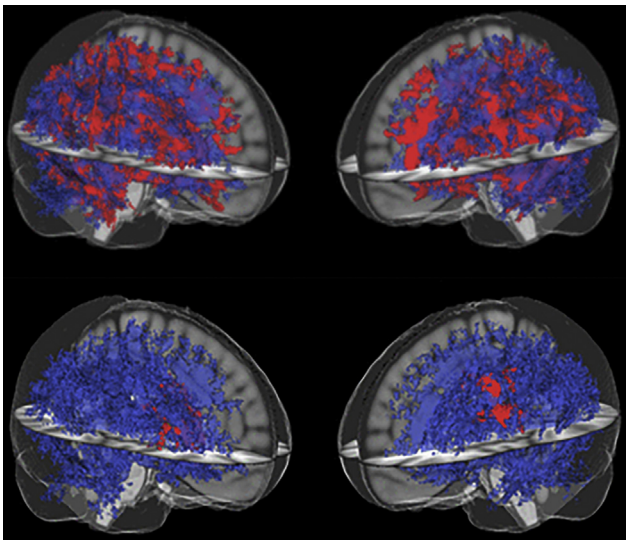

Figure 4. Imaging neuroinflammation with free-water imaging. The upper panel demonstrates a global patter of significantly decreased fractional anisotropy (red to yellow) and increased mean diffusivity (blue to dark blue) in patients with first-episode schizophrenia relative to healthy control subjects. The fractional anisotropy map is drawn on top of the mean diffusivity map. The lower panel shows a localized pattern of significantly decreased free-water–corrected fractional anisotropy (red to yellow) in frontal regions, and a global pattern of significantly increased free-water (blue to dark blue). The FA_T map is drawn on top of the free-water map. Figure adapted from Pasternak *et al.* (60).

evaluations of specific neuroinflammatory processes (see Figure 3). In line with this contention, orientation dispersion index has been confirmed to correspond well with histopathological microglia density (75). It may therefore be sensitive to microgliosis as opposed to providing a crude measure of neurite dispersion. Similarly, the associations between interferon alpha–induced fatigue and increased neurite density index may be explained by the fact that interferon alpha therapy increases glutaminergic activity and that within the brain, 50% of glucose consumption is accounted for by astrocytes (74). Astrocytic processes might therefore contribute to neurite density index. At this state, these are speculative interpretations. The computation of precise NODDI metrics requires multishell diffusion MRI acquisitions, making it impossible to apply this method retrospectively to older MRI studies, which typically used single-shell acquisitions. The uptake of multishell diffusion sequences in standard research protocols will likely result in an increase of NODDI studies in clinical populations. Combined with histopathological validations of neuroinflammation, these studies will be able to determine the usefulness of NODDI measures as neuroimaging markers of neuroinflammation.

Studies in Neurological Versus Psychiatric Disorders. Table 7 summarizes the number of studies reviewed that were conducted in neurological disorders not inflammatory in nature and psychiatric disorders using the MRI method. The majority of studies were conducted in neurological disorders (74%). No studies were identified that used magnetization transfer imaging or diffusion basis spectrum imaging, and our search did not detect any USPIO-based CE-MRI studies performed in psychiatric disorders.

DISCUSSION

Multiple MRI methods are converging on the important problem of noninvasive evaluation of inflammatory mechanisms. Currently, the two most promising approaches are novel contrast agents, particularly USPIOs, and biophysical diffusion compartment models. USPIO-enhanced MRI visualizes the neuroinflammatory process via contrast binding to macrophages that cross the BBB (76), which is particularly useful in neurological disorders involving trauma to the BBB, such as stroke and TBI. Emerging diffusion MRI protocols provide a complementary approach. Rather than being immune cell based, methods such as FW imaging and NODDI provide a detailed evaluation of the extraneuronal space. Astrocytes and microglia contribute to the microstructural configuration of this space and are key players in the initiation and modulation of immune defense in the brain. Specific features and compartments at the subvoxel scale may therefore prove to be highly sensitive to inflammation. With the continuous improvement of MRI sequences and their translation to clinical settings, these methods will likely continue to improve specificity and sensitivity to more subtle neuroinflammatory processes linked to psychiatric diseases and neurological disorders not involving BBB leakage.

Studies investigating neuroinflammation using MRI in neurological disorders outnumbered those conducted in psychiatric disorders. This is largely true for studies using CE-MRI methods. Approximately one third of identified studies used Gd-enhanced MRI to image inflammation-induced BBB leakage. Because Gd does not cross the healthy BBB, its application is particularly useful in classical neuroinflammatory disorders or neurological disorders that involve at least a temporary BBB opening, such as stroke and TBI. Psychiatric disorders, however, are not associated with changes in BBB permeability, making Gd-based CE-MRI less applicable to these cohorts. We were also unable to identify any studies that used USPIO enhancement to examine neuroinflammation in psychiatric disorders. Given the fact that USPIOs can cross the healthy BBB, we believe that this method has been understudied.

The validity of CE-MRI methods and MRI compartment models has been established immunohistochemically in animal models. While the immune systems of multicellular animals have evolved from common origins, several immune functions, especially those involving an adaptive immune response, differ quite drastically between species (77). Furthermore, BBB permeability varies extensively across vertebrates and primates, further complicating the generalizability of validation studies across species. While some studies included peripheral or CSF markers of inflammation (20,27,28,34,68,75,78), statistical comparisons were often not conducted (27,34) or did not generate evidence for an association between different modalities (75). Despite commonly reported associations between traditional diffusion tensor imaging metrics such as fractional anisotropy and inflammation markers from blood

Table 6. Studies in Neurological and Psychiatric Disorders Using NODDI to Study Neuroinflammation

Study	Sample	Design and Analysis	Results and Conclusions	Validation
Neurological Disorders: TBI/Concussion				
Churchill *et al.*, 2018 (70)	33 concussed athletes. 33 age- and gender-matched HC subjects.	MRI 1–7 days after concussion (SYM) and after medical clearance (RTP). Coregistration of dMRI to group template. FA, AD, RD, ODI, V_{ISO}, and V_{IC} from mask of voxels with FA $\geq$ 0.30. Voxelwise mean difference between SYM and HC subjects and longitudinal change from SYM to RTP. Multivariate NPLS test for WM regions with simultaneous effects of concussion for 6 DTI/NODDI measures.	Extensive decreases in FA and increases in AD and RD associated with reduced V_{IC}, at SYM and RTP, indicating that effects persist beyond medical clearance. Concussed athletes with higher symptom burden and a longer recovery time had FA reductions and AD, RD, and ODI increases. Presence of WM effects at RTP suggest a longer-term neurobiological response, such as neuroinflammation as opposed to neurodegeneration or tissue changes.	0
Wu *et al.*, 2018 (71)	19 patients with mTBI. 23 other trauma control subjects.	MRI within 15 days of brain injury. TBSS (MD, AD, RD, MD, V_{IC}, ODI, P_0).	V_{IC}: mTBI < trauma control subjects in CC and anterior and superior corona radiata. Higher V_{IC} and P_0 associated with better performances in trauma control subjects and worse performance in mTBI on measures of attention, memory, and executive function. Measures of axonal density are associated with cognitive performance. Inverse correlation in mTBI may be explained by association of axonal density with higher ratio of neurosupportive cells, such as astrocytes. Evidence suggests that astrocytes regulate and restrict inflammation and help preserve brain function after TBI.	0
Neurological Disorders: Alzheimer's Disease				
Metzler-Baddeley *et al.*, 2019 (72)	166 APOE genotyped healthy adults.	Tractography of parahippocampal cingulum, fornix, uncinate fasciculus (qMT: k_f, MPF; NODDI: ICSF, ODI, ISOSF). Blood sample (leptin, APN, CRP, IL-8). Obesity measures.	Obesity was negatively correlated with MPF and k_f but not with any NODDI measures. In men, differences in leptin/APN ratio fully mediated effect of obesity on fornix MPF. Visceral fat–related systemic inflammation may damage myelin properties of fornix, a limbic tract involved in late-onset Alzheimer's disease.	1: peripheral IL-8 was associated with qMT measures but not NODDI metrics. Results do not validate ICSF, ODI, or ISOSF as inflammation markers.
Psychiatric Disorders: Major Depressive Disorder				
Dowell *et al.*, 2019 (74)	18 patients with hepatitis C receiving IFN-α treatment.	MRI/blood (baseline, 4 hours after IFN-α). ROIs in striatum and insula (NDI). Psychological assessments over 12 weeks (depression [HAMD], fatigue). Blood (IFN-α and other cytokines).	IFN-α–induced acute increase in NDI in patients that experienced increase in IFN-α–induced fatigue. Acute changes in striatal microstructure predicted continued development of fatigue but not depression 4 and 8 weeks later. NODDI is a potential in vivo biomarker of the central effects of peripheral inflammation.	2: peripheral IFN- α was positively correlated with NDI, indicating that NDI might be sensitive to inflammation.

Table 6. Continued

Study	Sample	Design and Analysis	Results and Conclusions	Validation
Psychiatric Disorders: Schizophrenia				
Kraguljac *et al.*, 2019 (66)	42 patients with SZ (30 antipsychotic-naïve, 12 untreated). 42 matched HC subjects.	MRI before and after a 6-week trial of risperidone. Whole-brain voxelwise analysis with FW and ODI.	Unmedicated and antipsychotic-naïve patients with SZ increased ODI in posterior limb of the internal capsule. No group differences in voxelwise FW or whole-brain ODI. 6.3% increase in whole-brain FW in unmedicated SZ vs. HC subjects. No changes after risperidone treatment. Increased ODI interpreted as lesser fiber uniformity in this area. Increased FW may reflect dynamic imbalance of inflammatory pathways across SZ illness stages.	0

AD, axial diffusivity; APOE, apolipoprotein E; APN, adiponectin; CC, corpus callosum; CRP, C-reactive protein; dMRI, diffusion magnetic resonance imaging; DTI, diffusion tensor imaging; FA, fractional anisotropy; FW, free-water; HAMD, Hamilton Depression Rating Scale; HC, healthy control; ICSF, intracellular signal fraction; IFN-α, interferon alpha; IL-8, interleukin 8; ISOSF, isotropic signal fraction; k_f, forward exchange rate (neuroinflammation/mitochondrial metabolism); MD, mean diffusivity; MPF, macromolecular proton fraction; MRI, magnetic resonance imaging; mTBI, mild traumatic brain injury; NDI, neurite density index; NODDI, neurite orientation dispersion and density imaging; NPLS, N-way partial least squares; ODI, orientation dispersion index; P_0, zero displacement probability; qMT, quantitative magnetization transfer; RD, radial diffusivity; ROI, region of interest; RTP, return to play; SYM, symptomatic concussed athlete; SZ, schizophrenia; TBI, traumatic brain injury; TBSS, tract-based spatial statistics; V_{IC}, intracellular water in neurites; V_{ISO}, free-water contributed by cerebral spinal fluid; WM, white matter.

(78–89), CSF (81,90,91) or molecular imaging (92–95), correlations have been interpreted to reflect white matter damage as a secondary consequence of inflammation rather than inflammation per se. While traditional diffusion tensor imaging metrics were not designed to measure inflammation, it is important to consider that other measures validated via correlations with systemic or CSF markers of inflammation may also merely share covarying mechanisms as opposed to representing markers of inflammation themselves.

The central challenge for MRI is therefore to identify signal characteristics that show specificity for neuroinflammation. PET is currently regarded as the gold standard for in vivo imaging of neuroinflammation and is sometimes viewed as the only direct method available. However, currently available PET ligands do not target a molecular change that is specific to inflammation. The best-known family of ligands is associated with the expression of TSPO, a key protein of the outer mitochondrial membrane, which is mainly expressed in glial cells. However, TSPO is involved in additional cellular functions, such as cholesterol transport, steroid synthesis, mitochondrial respiration, proliferation, apoptosis, and tumorigenesis (96). Furthermore, while first-generation TSPO ligands alter their binding affinity with temperature changes and show a high level of nonspecific binding, second-generation ligands bind to targets other than TSPO, such as human constitutive androstane receptor (96). As such, TSPO expression represents as much an indirect measure of inflammation as biophysical changes measured by MRI. Moreover, methods such as USPIO-enhanced MRI offer the possibility of cell-specific MR contrast, which is another limitation of TSPO PET studies. By binding specifically to macrophages that cross the BBB (76), USPIOs facilitate comparable, if not better, results by harnessing the advantages of MRI. Novel USPIOs have been designed to target specific neuroinflammatory processes. While currently only available for preclinical research, many of these USPIOs have properties designed for clinical use in humans (97). A new class of superparamagnetic nanoparticles, anionic maghemite nanoparticles, are captured by cells with an efficiency three orders of magnitude higher than typical USPIOs such as ferumoxytol (98), enabling improved cell labeling across a wide variety of cells (99).

Table 7. Number of Studies Conducted in Neurological and Psychiatric Disorders Using the MRI Method

MRI Method	Neurology	Psychiatry
Gadolinium-Based CE-MRI	17	1
USPIO-Based CE-MRI	2	0
MTI	0	0
DKI	3	1
Free-Water Imaging	15	10
NODDI	3	2
D(B)SI	0	0
Total	40	14

CE-MRI, contrast-enhanced magnetic resonance imaging; D(B)SI, diffusion (basis) spectrum imaging; DKI, diffusion kurtosis imaging; MRI, magnetic resonance imaging; MTI, magnetization transfer imaging; NODDI, neurite orientation dispersion and density imaging; USPIO, ultrasmall superparamagnetic particles of iron oxide.

Emerging Techniques and Future Perspectives

Convergent information including biochemical, molecular, and biophysical perspectives, from a combination of PET and MR techniques, may be a promising approach to characterize inflammatory processes in the brain. Evaluating USPIO-based

MRI and PET in parallel would offer the opportunity to evaluate the extent to which neuroinflammatory processes imaged by either method are suitable to detect inflammation across different neurological and psychiatric disorders. Advances in diffusion MRI produce detailed insights into tissue compartments that yield more realistic biophysical models, are sensitive to subtle tissue changes in the absence of BBB disruptions, and do not require the administration of contrast agents, making them the ideal candidate to aid interpretation of PET and USPIO-based MRI results. Multimodal validation studies will also be able to determine whether compartment models map onto cellular or molecular inflammatory processes, such as macrophage infiltration imaged by USPIOs. In humans, multimodal imaging studies with neuropathological validation are a priority for making progress in this field. Using typhoid and viral mimetic approaches to validate MRI markers of neuroinflammation (100), a favored approach to date, is problematic because these approaches induce a short-lived, systemic immune response, which is not a realistic model of neuroinflammation found in neurological or psychiatric disease. MRI markers of neuroinflammation that have been validated in preclinical models therefore need to be evaluated immunohistochemically in postmortem tissue from humans. An additional important consideration for future studies is the collection of CSF. CSF sampling involves an invasive procedure, possibly not well tolerated by some participants. However, it offers the advantage of estimating inflammatory markers in the CNS as opposed to peripheral markers collected via blood samples.

Contrast agents targeting integrin $\alpha v\beta 3$ represent another encouraging area for noninvasive CE-MRI of neuroinflammation. Integrins are cell surface receptors that interact with inflamed endothelium and stromal extracellular matrix components to facilitate migration of cells into inflamed tissue (13). Specifically, integrin $\alpha v\beta 3$ is a cell adhesion molecule that is expressed on endothelial cells, macrophages, and platelets (13). It is expressed in high levels in inflammatory T helper type 17 cells required for cell-mediated autoimmune inflammation of the nervous system (101). The tripeptides RGD, which contain the 3-amino acid sequence arginine-glycine-aspartic acid, are ligands for integrin $\alpha v\beta 3$ and can be conjugated to Gd-based paramagnetic nanoparticles (102) and USPIO-based superparamagnetic nanoparticles (103). In humans, molecular imaging and immunochemistry expression of integrin $\alpha v\beta 3$ are highly correlated. Together with its superior resolution, MRI of neuroinflammation with RGD peptides represents a candidate with high translational potential to clinical settings. Rapid advances in nanotechnology and promising preclinical findings will likely push CE-MRI to the forefront of MRI methods used to study neuroinflammation in humans transdiagnostically.

In summary, with accumulating evidence suggesting that neuroinflammation plays a major role in the development and progression of neurological disorders not typically classified as neuroinflammatory in nature (10) and psychiatric disorders (11), the need to identify neuroinflammation early is becoming increasingly apparent. The continuous improvement of MRI hardware capabilities, together with the development of new contrast agents, validation studies of diffusion multicompartment models in humans, and increasing accessibility, affordability, and harmonization of large-scale MRI datasets will undoubtedly pave the way to establish reliable MRI markers of neuroinflammation. This will offer a cost-efficient and readily available tool to identify neuroinflammation transdiagnostically, which in turn may open the opportunity for early interventions to limit illness progression and prevent chronic microstructural tissue loss.

ACKNOWLEDGMENTS AND DISCLOSURES

This study was funded by the Medical Research Council, United Kingdom (Grant No. MR/K022113/1) and the European Commission Horizon 2020 Health Programme (CoSTREAM, Grant No. 667375 [to MJO]. LO is supported by an Emerging Leadership Fellowship from the National Health and Medical Research Council of Australia (Grant No. 2021/GNT2007718).

MJO has received support to attend meetings from Boehringer Ingelheim and received honoraria for consultancy from EMVison Medical Devices Ltd, Australia. LKLO reports no biomedical financial interests or potential conflicts of interest.

ARTICLE INFORMATION

From the Centre for Clinical Research (LKLO, MJO), Centre for Advanced Imaging (LKLO), and Institute of Molecular Bioscience (MJO), The University of Queensland; and the Department of Neurology (MJO), Royal Brisbane and Women's Hospital, Brisbane, Queensland, Australia.

Address correspondence to Lena K.L. Oestreich, Ph.D., at l.oestreich@uq.edu.au.

Received Sep 7, 2021; revised Jan 3, 2022; accepted Jan 4, 2022.

Supplementary material cited in this article is available online at https://doi.org/10.1016/j.bpsc.2022.01.003.

REFERENCES

1. Khansari PS, Sperlagh B (2012): Inflammation in neurological and psychiatric diseases. Inflammopharmacology 20:103–107.
2. Wunder A, Klohs J, Dirnagl U (2009): Non-invasive visualization of CNS inflammation with nuclear and optical imaging. Neuroscience 158:1161–1173.
3. Skaper SD, Facci L, Zusso M, Giusti P (2018): An inflammation-centric view of neurological disease: Beyond the neuron [published correction appears in Front Cell Neurosci 2020; 13:578]. Front Cell Neurosci 12:72.
4. Piirainen S, Youssef A, Song C, Kalueff AV, Landreth GE, Malm T, Tian L (2017): Psychosocial stress on neuroinflammation and cognitive dysfunctions in Alzheimer's disease: The emerging role for microglia? Neurosci Biobehav Rev 77:148–164.
5. Pasternak O, Kubicki M, Shenton ME (2016): In vivo imaging of neuroinflammation in schizophrenia. Schizophr Res 173:200–212.
6. da Fonseca ACC, Matias D, Garcia C, Amaral R, Geraldo LH, Freitas C, Lima FRS (2014): The impact of microglial activation on blood-brain barrier in brain diseases. Front Cell Neurosci 8:362.
7. Takeshita Y, Ransohoff RM (2012): Inflammatory cell trafficking across the blood-brain barrier: Chemokine regulation and in vitro models. Immunol Rev 248:228–239.
8. Quarantelli M (2015): MRI/MRS in neuroinflammation: Methodology and applications. Clin Transl Imaging 3:475–489.
9. Thiel A, Radlinska BA, Paquette C, Sidel M, Soucy JP, Schirrmacher R, Minuk J (2010): The temporal dynamics of post-stroke neuroinflammation: A longitudinal diffusion tensor imaging-guided PET study with 11C-PK11195 in acute subcortical stroke. J Nucl Med 51:1404–1412.
10. Degan D, Ornello R, Tiseo C, Carolei A, Sacco S, Pistoia F (2018): The role of inflammation in neurological disorders. Curr Pharm Des 24:1485–1501.

11. Lurie DI (2018): An integrative approach to neuroinflammation in psychiatric disorders and neuropathic pain. J Exp Neurosci 12: 1179069518793639.
12. Hesdorffer DC (2016): Comorbidity between neurological illness and psychiatric disorders. CNS Spectr 21:230–238.
13. Pulli B, Chen JW (2014): Imaging neuroinflammation—From bench to bedside. J Clin Cell Immunol 5:226.
14. Ford AL, An H, D'Angelo G, Ponisio R, Bushard P, Vo KD, *et al.* (2011): Preexisting statin use is associated with greater reperfusion in hyperacute ischemic stroke. Stroke 42:1307–1313.
15. Qiao Y, Zeiler SR, Mirbagheri S, Leigh R, Urrutia V, Wityk R, Wasserman BA (2014): Intracranial plaque enhancement in patients with cerebrovascular events on high-spatial-resolution MR images. Radiology 271:534–542.
16. Qiao Y, Etesami M, Astor BC, Zeiler SR, Trout HH 3rd, Wasserman BA (2012): Carotid plaque neovascularization and hemorrhage detected by MR imaging are associated with recent cerebrovascular ischemic events. AJNR Am J Neuroradiol 33:755–760.
17. Natori T, Sasaki M, Miyoshi M, Ito K, Ohba H, Miyazawa H, *et al.* (2016): Intracranial plaque characterization in patients with acute ischemic stroke using pre- and post-contrast three-dimensional magnetic resonance vessel wall imaging. J Stroke Cerebrovasc Dis 25:1425–1430.
18. Choi HY, Lee KM, Kim HG, Kim EJ, Choi WS, Kim BJ, *et al.* (2017): Role of hyperintense acute reperfusion marker for classifying the stroke etiology. Front Neurol 8:630.
19. Wardlaw JM, Makin SJ, Valdés Hernández MC, Armitage PA, Heye AK, Chappell FM, *et al.* (2017): Blood-brain barrier failure as a core mechanism in cerebral small vessel disease and dementia: Evidence from a cohort study. Alzheimers Dement 13:634–643.
20. Arba F, Leigh R, Inzitari D, Warach SJ, Luby M, Lees KR, STIR/VISTA Imaging Collaboration (2017): Blood-brain barrier leakage increases with small vessel disease in acute ischemic stroke. Neurology 89:2143–2150.
21. O'Connell GC, Treadway MB, Petrone AB, Tennant CS, Lucke-Wold N, Chantler PD, Barr TL (2017): Peripheral blood AKAP7 expression as an early marker for lymphocyte-mediated post-stroke blood brain barrier disruption. Sci Rep 7:1172.
22. Gupta N, Simpkins AN, Hitomi E, Dias C, Leigh R, NIH Natural History of Stroke Investigators (2018): White matter hyperintensity-associated blood-brain barrier disruption and vascular risk factors. J Stroke Cerebrovasc Dis 27:466–471.
23. Nadareishvili Z, Luby M, Leigh R, Shah J, Lynch JK, Hsia AW, *et al.* (2018): An MRI hyperintense acute reperfusion marker is related to elevated peripheral monocyte count in acute ischemic stroke. J Neuroimaging 28:57–60.
24. Rost NS, Cougo P, Lorenzano S, Li H, Cloonan L, Bouts MJ, *et al.* (2018): Diffuse microvascular dysfunction and loss of white matter integrity predict poor outcomes in patients with acute ischemic stroke. J Cereb Blood Flow Metab 38:75–86.
25. Wu F, Ma Q, Song H, Guo X, Diniz MA, Song SS, *et al.* (2018): Differential features of culprit intracranial atherosclerotic lesions: A whole-brain vessel wall imaging study in patients with acute ischemic stroke. J Am Heart Assoc 7:e009705.
26. Lublinsky S, Major S, Kola V, Horst V, Santos E, Platz J, *et al.* (2019): Early blood-brain barrier dysfunction predicts neurological outcome following aneurysmal subarachnoid hemorrhage. EBioMedicine 43:460–472.
27. Nadareishvili Z, Simpkins AN, Hitomi E, Reyes D, Leigh R (2019): Post-stroke blood-brain barrier disruption and poor functional outcome in patients receiving thrombolytic therapy. Cerebrovasc Dis 47:135–142.
28. Cho YE, Latour LL, Kim H, Turtzo LC, Olivera A, Livingston WS, *et al.* (2016): Older age results in differential gene expression after mild traumatic brain injury and is linked to imaging differences at acute follow-up. Front Aging Neurosci 8:168.
29. Livingston WS, Gill JM, Cota MR, Olivera A, O'Keefe JL, Martin C, Latour LL (2017): Differential gene expression associated with meningeal injury in acute mild traumatic brain injury. J Neurotrauma 34:853–860.
30. Ding XB, Wang XX, Xia DH, Liu H, Tian HY, Fu Y, *et al.* (2021): Impaired meningeal lymphatic drainage in patients with idiopathic Parkinson's disease. Nat Med 27:411–418.
31. Kallaur AP, Lopes J, Oliveira SR, Simão ANC, Reiche EMV, de Almeida ERD, *et al.* (2016): Immune-inflammatory and oxidative and nitrosative stress biomarkers of depression symptoms in subjects with multiple sclerosis: Increased peripheral inflammation but less acute neuroinflammation. Mol Neurobiol 53:5191–5202.
32. Thrippleton MJ, Blair GW, Valdes-Hernandez MC, Glatz A, Semple SIK, Doubal F, *et al.* (2019): MRI relaxometry for quantitative analysis of USPIO uptake in cerebral small vessel disease. Int J Mol Sci 20:776.
33. Khan S, Amin FM, Fliedner FP, Christensen CE, Tolnai D, Younis S, *et al.* (2019): Investigating macrophage-mediated inflammation in migraine using ultrasmall superparamagnetic iron oxide-enhanced 3T magnetic resonance imaging. Cephalalgia 39:1407–1420.
34. Grossman EJ, Jensen JH, Babb JS, Chen Q, Tabesh A, Fieremans E, *et al.* (2013): Cognitive impairment in mild traumatic brain injury: A longitudinal diffusional kurtosis and perfusion imaging study. AJNR Am J Neuroradiol 34:951–957,S1–S3.
35. Fieremans E, Benitez A, Jensen JH, Falangola MF, Tabesh A, Deardorff RL, *et al.* (2013): Novel white matter tract integrity metrics sensitive to Alzheimer disease progression. AJNR Am J Neuroradiol 34:2105–2112.
36. Dong JW, Jelescu IO, Ades-Aron B, Novikov DS, Friedman K, Babb JS, *et al.* (2020): Diffusion MRI biomarkers of white matter microstructure vary nonmonotonically with increasing cerebral amyloid deposition. Neurobiol Aging 89:118–128.
37. McKenna FF, Miles L, Babb JS, Goff DC, Lazar M (2019): Diffusion kurtosis imaging of gray matter in schizophrenia. Cortex 121:201–224.
38. Ismail R, Parbo P, Madsen LS, Hansen AK, Hansen KV, Schaldemose JL, *et al.* (2020): The relationships between neuroinflammation, beta-amyloid and tau deposition in Alzheimer's disease: A longitudinal PET study. J Neuroinflammation 17:151.
39. Archer DB, Patten C, Coombes SA (2017): Free-water and free-water corrected fractional anisotropy in primary and premotor corticospinal tracts in chronic stroke. Hum Brain Mapp 38:4546–4562.
40. Duering M, Finsterwalder S, Baykara E, Tuladhar AM, Gesierich B, Konieczny MJ, *et al.* (2018): Free water determines diffusion alterations and clinical status in cerebral small vessel disease. Alzheimers Dement 14:764–774.
41. Oestreich LKL, Wright P, O'Sullivan MJ (2020): Microstructural changes in the reward system are associated with post-stroke depression. Neuroimage Clin 28:102360.
42. Pasternak O, Koerte IK, Bouix S, Fredman E, Sasaki T, Mayinger M, *et al.* (2014): Hockey Concussion Education Project, Part 2. Microstructural white matter alterations in acutely concussed ice hockey players: A longitudinal free-water MRI study [published correction appears in J Neurosurg 2014; 121:498–500]. J Neurosurg 120:873–881.
43. Hoy AR, Ly M, Carlsson CM, Okonkwo OC, Zetterberg H, Blennow K, *et al.* (2017): Microstructural white matter alterations in preclinical Alzheimer's disease detected using free water elimination diffusion tensor imaging. PLoS One 12:e0173982.
44. Ji F, Pasternak O, Liu S, Loke YM, Choo BL, Hilal S, *et al.* (2017): Distinct white matter microstructural abnormalities and extracellular water increases relate to cognitive impairment in Alzheimer's disease with and without cerebrovascular disease. Alzheimers Res Ther 9:63.
45. Montal V, Vilaplana E, Alcolea D, Pegueroles J, Pasternak O, González-Ortiz S, *et al.* (2018): Cortical microstructural changes along the Alzheimer's disease continuum. Alzheimers Dement 14:340–351.
46. Ofori E, DeKosky ST, Febo M, Colon-Perez L, Chakrabarty P, Duara R, *et al.* (2019): Free-water imaging of the hippocampus is a sensitive marker of Alzheimer's disease. Neuroimage Clin 24:101985.

47. Archer DB, Coombes SA, McFarland NR, DeKosky ST, Vaillancourt DE (2019): Development of a transcallosal tractography template and its application to dementia. Neuroimage 200:302–312.
48. Vipin A, Ng KK, Ji F, Shim HY, Lim JKW, Pasternak O, *et al.* (2019): Amyloid burden accelerates white matter degradation in cognitively normal elderly individuals. Hum Brain Mapp 40:2065–2075.
49. Ji F, Pasternak O, Ng KK, Chong JSX, Liu S, Zhang L, *et al.* (2019): White matter microstructural abnormalities and default network degeneration are associated with early memory deficit in Alzheimer's disease continuum. Sci Rep 9:4749.
50. Ofori E, Pasternak O, Planetta PJ, Burciu R, Snyder A, Febo M, *et al.* (2015): Increased free water in the substantia nigra of Parkinson's disease: A single-site and multi-site study. Neurobiol Aging 36:1097–1104.
51. Ofori E, Krismer F, Burciu RG, Pasternak O, McCracken JL, Lewis MM, *et al.* (2017): Free water improves detection of changes in the substantia nigra in parkinsonism: A multisite study. Mov Disord 32:1457–1464.
52. Guttuso T Jr, Bergsland N, Hagemeier J, Lichter DG, Pasternak O, Zivadinov R (2018): Substantia nigra free water increases longitudinally in Parkinson disease. AJNR Am J Neuroradiol 39:479–484.
53. Andica C, Kamagata K, Hatano T, Saito A, Uchida W, Ogawa T, *et al.* (2019): Free-water imaging in white and gray matter in Parkinson's disease. Cells 8:839.
54. Braak H, Braak E (1998): Evolution of neuronal changes in the course of Alzheimer's disease. J Neural Transm Suppl 53:127–140.
55. Perez-Nievas BG, Stein TD, Tai HC, Dols-Icardo O, Scotton TC, Barroeta-Espar I, *et al.* (2013): Dissecting phenotypic traits linked to human resilience to Alzheimer's pathology. Brain 136:2510–2526.
56. Planetta PJ, Ofori E, Pasternak O, Burciu RG, Shukla P, DeSimone JC, *et al.* (2016): Free-water imaging in Parkinson's disease and atypical parkinsonism. Brain 139:495–508.
57. Streit WJ (2006): Microglial senescence: Does the brain's immune system have an expiration date? Trends Neurosci 29:506–510.
58. Bergamino M, Pasternak O, Farmer M, Shenton ME, Hamilton JP (2015): Applying a free-water correction to diffusion imaging data uncovers stress-related neural pathology in depression. Neuroimage Clin 10:336–342.
59. Tuozzo C, Lyall AE, Pasternak O, James ACD, Crow TJ, Kubicki M (2018): Patients with chronic bipolar disorder exhibit widespread increases in extracellular free water. Bipolar Disord 20:523–530.
60. Pasternak O, Westin CF, Bouix S, Seidman LJ, Goldstein JM, Woo TUW, *et al.* (2012): Excessive extracellular volume reveals a neurodegenerative pattern in schizophrenia onset. J Neurosci 32:17365–17372.
61. Pasternak O, Westin CF, Dahlben B, Bouix S, Kubicki M (2015): The extent of diffusion MRI markers of neuroinflammation and white matter deterioration in chronic schizophrenia. Schizophr Res 161:113–118.
62. Oestreich LKL, Lyall AE, Pasternak O, Kikinis Z, Newell DT, Savadjiev P, *et al.* (2017): Characterizing white matter changes in chronic schizophrenia: A free-water imaging multi-site study. Schizophr Res 189:153–161.
63. Oestreich LKL, Pasternak O, Shenton ME, Kubicki M, Gong X, Australian Schizophrenia Research Bank, *et al.* (2016): Abnormal white matter microstructure and increased extracellular free-water in the cingulum bundle associated with delusions in chronic schizophrenia. Neuroimage Clin 12:405–414.
64. Lyall AE, Pasternak O, Robinson DG, Newell D, Trampush JW, Gallego JA, *et al.* (2018): Greater extracellular free-water in first-episode psychosis predicts better neurocognitive functioning. Mol Psychiatry 23:701–707.
65. Di Biase MA, Zalesky A, Cetin-Karayumak S, Rathi Y, Lv J, Boerrigter D, *et al.* (2021): Large-scale evidence for an association between peripheral inflammation and white matter free water in schizophrenia and healthy individuals. Schizophr Bull 47:542–551.
66. Kraguljac NV, Anthony T, Monroe WS, Skidmore FM, Morgan CJ, White DM, *et al.* (2019): A longitudinal neurite and free water imaging study in patients with a schizophrenia spectrum disorder. Neuropsychopharmacology 44:1932–1939.
67. Tang Y, Pasternak O, Kubicki M, Rathi Y, Zhang T, Wang J, *et al.* (2019): Altered cellular white matter but not extracellular free water on diffusion MRI in individuals at clinical high risk for psychosis. Am J Psychiatry 176:820–828.
68. Bullmore E (2018): The Inflamed Mind: A Radical New Approach to Depression. London, United Kingdom: Short Books Book Company Ltd.
69. Di Biase MA, Katabi G, Piontkewitz Y, Cetin-Karayumak S, Weiner I, Pasternak O (2020): Increased extracellular free-water in adult male rats following in utero exposure to maternal immune activation. Brain Behav Immun 83:283–287.
70. Churchill NW, Caverzasi E, Graham SJ, Hutchison MG, Schweizer TA (2019): White matter during concussion recovery: Comparing diffusion tensor imaging (DTI) and neurite orientation dispersion and density imaging (NODDI). Hum Brain Mapp 40:1908–1918.
71. Wu YC, Mustafi SM, Harezlak J, Kodiweera C, Flashman LA, McAllister TW (2018): Hybrid diffusion imaging in mild traumatic brain injury. J Neurotrauma 35:2377–2390.
72. Metzler-Baddeley C, Mole JP, Leonaviciute E, Sims R, Kidd EJ, Ertefai B, *et al.* (2019): Sex-specific effects of central adiposity and inflammatory markers on limbic microstructure. Neuroimage 189:793–803.
73. Reid MA, White DM, Kraguljac NV, Lahti AC (2016): A combined diffusion tensor imaging and magnetic resonance spectroscopy study of patients with schizophrenia. Schizophr Res 170:341–350.
74. Dowell NG, Bouyagoub S, Tibble J, Voon V, Cercignani M, Harrison NA (2019): Interferon-alpha-induced changes in NODDI predispose to the development of fatigue. Neuroscience 403:111–117.
75. Yi SY, Barnett BR, Torres-Velázquez M, Zhang Y, Hurley SA, Rowley PA, *et al.* (2019): Detecting microglial density with quantitative multi-compartment diffusion MRI. Front Neurosci 13:81.
76. Deddens LH, Van Tilborg GAF, Mulder WJM, De Vries HE, Dijkhuizen RM (2012): Imaging neuroinflammation after stroke: Current status of cellular and molecular MRI strategies. Cerebrovasc Dis 33:392–402.
77. Bailey M, Christoforidou Z, Lewis MC (2013): The evolutionary basis for differences between the immune systems of man, mouse, pig and ruminants. Vet Immunol Immunopathol 152(1–2):13–19.
78. Walker KA, Power MC, Hoogeveen RC, Folsom AR, Ballantyne CM, Knopman DS, *et al.* (2017): Midlife systemic inflammation, late-life white matter integrity, and cerebral small vessel disease: The Atherosclerosis Risk in Communities Study. Stroke 48:3196–3202.
79. Besga A, Chyzhyk D, Gonzalez-Ortega I, Echeveste J, Grana-Lecuona M, Grana M, *et al.* (2017): White matter tract integrity in Alzheimer's disease vs. late onset bipolar disorder and its correlation with systemic inflammation and oxidative stress biomarkers. Front Aging Neurosci 9:179.
80. Cox CS Jr, Hetz RA, Liao GP, Aertker BM, Ewing-Cobbs L, Juranek J, *et al.* (2017): Treatment of severe adult traumatic brain injury using bone marrow mononuclear cells. Stem Cells 35:1065–1079.
81. Lueg G, Gross CC, Lohmann H, Johnen A, Kemmling A, Deppe M, *et al.* (2015): Clinical relevance of specific T-cell activation in the blood and cerebrospinal fluid of patients with mild Alzheimer's disease. Neurobiol Aging 36:81–89.
82. Chiang PL, Chen HL, Lu CH, Chen PC, Chen MH, Yang IH, *et al.* (2017): White matter damage and systemic inflammation in Parkinson's disease. BMC Neurosci 18:48.
83. Sugimoto K, Kakeda S, Watanabe K, Katsuki A, Ueda I, Igata N, *et al.* (2018): Relationship between white matter integrity and serum inflammatory cytokine levels in drug-naive patients with major depressive disorder: Diffusion tensor imaging study using tract-based spatial statistics. Transl Psychiatry 8:141.

84. Lotrich FE, Butters MA, Aizenstein H, Marron MM, Reynolds CF 3rd, Gildengers AG (2014): The relationship between interleukin-1 receptor antagonist and cognitive function in older adults with bipolar disorder. Int J Geriatr Psychiatry 29:635–644.
85. Benedetti F, Poletti S, Hoogenboezem TA, Mazza E, Ambree O, de Wit H, *et al.* (2016): Inflammatory cytokines influence measures of white matter integrity in bipolar disorder. J Affect Disord 202: 1–9.
86. Poletti S, de Wit H, Mazza E, Wijkhuijs AJM, Locatelli C, Aggio V, *et al.* (2017): Th17 cells correlate positively to the structural and functional integrity of the brain in bipolar depression and healthy controls. Brain Behav Immun 61:317–325.
87. Mäntylä T, Mantere O, Raij TT, Kieseppä T, Laitinen H, Leiviskä J, *et al.* (2015): Altered activation of innate immunity associates with white matter volume and diffusion in first-episode psychosis. PLoS One 10:e0125112.
88. Prasad KM, Upton CH, Nimgaonkar VL, Keshavan MS (2015): Differential susceptibility of white matter tracts to inflammatory mediators in schizophrenia: An integrated DTI study. Schizophr Res 161:119–125.
89. Fu G, Zhang W, Dai J, Liu J, Li F, Wu D, *et al.* (2019): Increased peripheral interleukin 10 relate to white matter integrity in schizophrenia. Front Neurosci 13:52.
90. Melah KE, Lu SY, Hoscheidt SM, Alexander AL, Adluru N, Destiche DJ, *et al.* (2016): Cerebrospinal fluid markers of Alzheimer's disease pathology and microglial activation are associated with altered white matter microstructure in asymptomatic adults at risk for Alzheimer's disease. J Alzheimers Dis 50:873–886.
91. Racine AM, Merluzzi AP, Adluru N, Norton D, Koscik RL, Clark LR, *et al.* (2019): Association of longitudinal white matter degeneration and cerebrospinal fluid biomarkers of neurodegeneration, inflammation and Alzheimer's disease in late-middle-aged adults. Brain Imaging Behav 13:41–52.
92. Ramlackhansingh AF, Brooks DJ, Greenwood RJ, Bose SK, Turkheimer FE, Kinnunen KM, *et al.* (2011): Inflammation after trauma: microglial activation and traumatic brain injury. Ann Neurol 70:374–383.
93. Dennis EL, Babikian T, Alger J, Rashid F, Villalon-Reina JE, Jin Y, *et al.* (2018): Magnetic resonance spectroscopy of fiber tracts in children with traumatic brain injury: A combined MRS - Diffusion MRI study. Hum Brain Mapp 39:3759–3768.
94. Alshikho MJ, Zürcher NR, Loggia ML, Cernasov P, Chonde DB, Izquierdo Garcia D, *et al.* (2016): Glial activation colocalizes with structural abnormalities in amyotrophic lateral sclerosis. Neurology 87:2554–2561.
95. Chiappelli J, Hong LE, Wijtenburg SA, Du X, Gaston F, Kochunov P, *et al.* (2015): Alterations in frontal white matter neurochemistry and microstructure in schizophrenia: Implications for neuroinflammation. Transl Psychiatry 5:e548.
96. Lee Y, Park Y, Nam H, Lee JW, Yu SW (2020): Translocator protein (TSPO): The new story of the old protein in neuroinflammation. BMB Rep 53:20–27.
97. Sigovan M, Boussel L, Sulaiman A, Sappey-Marinier D, Alsaid H, Desbleds-Mansard C, *et al.* (2009): Rapid-clearance iron nanoparticles for inflammation imaging of atherosclerotic plaque: Initial experience in animal model. Radiology 252:401–409.
98. Wilhelm C, Billotey C, Roger J, Pons JN, Bacri JC, Gazeau F (2003): Intracellular uptake of anionic superparamagnetic nanoparticles as a function of their surface coating. Biomaterials 24:1001–1011.
99. Brisset JC, Desestret V, Marcellino S, Devillard E, Chauveau F, Lagarde F, *et al.* (2010): Quantitative effects of cell internalization of two types of ultrasmall superparamagnetic iron oxide nanoparticles at 4.7 T and 7 T. Eur Radiol 20:275–285.
100. Harrison NA, Cooper E, Dowell NG, Keramida G, Voon V, Critchley HD, Cercignani M (2015): Quantitative magnetization transfer imaging as a biomarker for effects of systemic inflammation on the brain. Biol Psychiatry 78:49–57.
101. Du F, Garg AV, Kosar K, Majumder S, Kugler DG, Mir GH, *et al.* (2016): Inflammatory Th17 cells express integrin $\alpha v\beta 3$ for pathogenic function. Cell Rep 16:1339–1351.
102. Schmieder AH, Winter PM, Caruthers SD, Harris TD, Williams TA, Allen JS, *et al.* (2005): Molecular MR imaging of melanoma angiogenesis with alphanubeta3-targeted paramagnetic nanoparticles. Magn Reson Med 53:621–627.
103. Zhang C, Jugold M, Woenne EC, Lammers T, Morgenstern B, Mueller MM, *et al.* (2007): Specific targeting of tumor angiogenesis by RGD-conjugated ultrasmall superparamagnetic iron oxide particles using a clinical 1.5-T magnetic resonance scanner. Cancer Res 67:1555–1562.